Kairos Power

KP-NRC-2006-004

June 30, 2020

Project No. 99902069

US Nuclear Regulatory Commission
ATTN: Document Control Desk
Washington, DC 20555-0001

Subject: Kairos Power LLC
Topical Report Submittal
Metallic Materials Qualification for the Kairos Power Fluoride Salt-Cooled, High Temperature Reactor

This letter submits the subject topical report which provides the Metallic Materials Qualification for the Kairos Power Fluoride Salt-Cooled, High Temperature Reactor (KP-FHR). This topical report is provided for NRC review and approval and is expected to be referenced by future license applicants using the KP-FHR. The scope and schedule for submittal of this report was discussed in a closed meeting with NRC staff on June 19, 2020. Kairos Power respectfully requests NRC acceptance review be completed and a review schedule be provided within 60 days of the receipt of this letter. In recognition of an aggressive deployment schedule and substantial pre-application engagement, Kairos Power has established a generic assumption of a 12-month review for topical reports.

Portions of the attached report are considered proprietary, and Kairos Power requests it be withheld from public disclosure in accordance with the provisions of 10 CFR 2.390. Enclosure 1 provides the proprietary version of the report and Enclosure 2 provides the non-proprietary report. An affidavit supporting the withholding request is provided in Enclosure 3.

Additionally, the information indicated as proprietary has also been determined to contain Export Controlled Information. This information must be protected from disclosure pursuant to the requirements of 10 CFR 810.

If you have any questions or need any additional information, please contact John Price at price@kairospower.com or (510) 808-5265, or Darrell Gardner at gardner@kairospower.com or (704) 769-1226.

Sincerely,

Peter Hastings, PE
Vice President, Regulatory Affairs and Quality

Enclosure:

1) Metallic Materials Qualification for the Kairos Power Testing Program (Proprietary)
2) Metallic Materials Qualification for the Kairos Power Testing Program (Non-Proprietary)
3) Affidavit Supporting Request for Withholding from Public Disclosure (10 CFR 2.390)

xc (w/enclosure):

Benjamin Beasley, Chief, Advanced Reactor Licensing Branch
Stewart Magruder, Project Manager, Advanced Reactor Licensing Branch

Enclosure 2

Metallic Materials Qualification for the Kairos Power Testing Program

(Non-Proprietary)

KP-TR-013-NP

Kairos Power LLC
707 W. Tower Ave
Alameda, CA 94501

Metallic Materials Qualification for the Kairos Power Fluoride Salt-Cooled High-Temperature Reactor

Topical Report

Revision No. 0
Document Date: June 2020

COPYRIGHT Notice

Rev	Description of Change	Date
0	Initial Issuance	June 2020

EXECUTIVE SUMMARY

This Topical Report describes the qualification plans for structural alloys used in the safety-related systems of the Kairos Power Fluoride Salt-Cooled, High Temperature Reactor (KP-FHR). The KP-FHR is an advanced Generation IV nuclear reactor being developed for U.S. commercial power generation. The reactor operates near atmospheric pressure and utilizes high temperature fuel and molten salt coolants to provide a high degree of passive safety.

This document describes the testing and modelling required to qualify the structural alloy materials used in the safety-related portion of the KP-FHR plant, i.e. the fluoride salt cooled primary heat transport system. In the primary heat transport system, [[

]]. This report does not describe material qualification for non-safety related systems. Specifically, this report describes work to extend the ASME qualification of structural alloys to higher temperatures and to demonstrate environmental compatibility of the structural materials for use in the KP-FHR. Additionally, this report presents, for information, ongoing work to develop coatings and cladding and reliability and integrity management plans for the KP-FHR.

Kairos Power is requesting Nuclear Regulatory Commission review and approval of the qualification plan described in this report for metallic structural materials used in Flibe wetted areas for safety-significant high temperature components of the KP-FHR for use by licensing applicants under 10 CFR 50 or 10 CFR 52.

Table of Contents

LIST OF ABBREVIATIONS

Acronym	Definition
ASME	American Society for Mechanical Engineers
ASTM	American Society for Testing and Materials
BWR	Boiling Water Reactor
CFR	Code of Federal Regulations
DPA	Displacements per Atom
DOE	Department of Energy
EAC	Environmentally Assisted Cracking
FHR	Fluoride Salt-Cooled High Temperature Reactor
FSAR	Final Safety Analysis Report
HFIR	High Flux Isotope Reactor
IASCC	Irradiation-Assisted Stress Corrosion Cracking
IGSCC	Intergranular Stress Corrosion Cracking
KP-FHR	Kairos Power Fluoride Salt-Cooled, High Temperature Reactor
LWA	Limited Work Authorization
LWR	Light Water Reactors
MANDE	Monitoring and Non-Destructive Examination
MHTGR	Modular High Temperature Gas Reactor
MSR	Molten Salt Reactor
MSRE	Molten Salt Reactor Experiment
NRC	Nuclear Regulatory Commission
OFHC	Oxygen-Free, High-Conductivity
ORNL	Oak Ridge National Laboratory
PDC	Principal Design Criteria
PIRT	Phenomena Identification and Ranking Table
PSAR	Preliminary Safety Analysis Report
PWR	Pressurized Water Reactor
RCL	Rotating Cage Loop
RG	Regulatory Guide
RIM	Reliability and Integrity Management
SCC	Stress Corrosion Cracking
SFR	Sodium-Cooled Fast Reactor
SSC	Structure, System, or Component
SSRT	Slow Strain Rate Testing
TRISO	Tri-Structural Isotropic

1 INTRODUCTION

Kairos Power LLC (Kairos Power) is pursuing the design, licensing, and deployment of a Fluoride Salt-Cooled, High Temperature Reactor, i.e. the KP-FHR. To support these objectives, Kairos Power will rely on the use of qualified high temperature metallic structural materials. The materials qualification program relies on both materials testing and modeling to ensure the performance of the safety-related metallic structural materials. This report details the approach for safety-related metallic structural materials qualification in Flibe wetted areas for the KP-FHR consistent with American Society of Mechanical Engineers (ASME) Section III Division 5 requirements.

The structural alloys for use in the KP-FHR were selected considering the commercial availability and if the material is qualified for use via ASME Section III Division 5 (Rules for Construction of Nuclear Power Plant Components, High Temperature Reactors). These rules for construction require demonstration of the environmental compatibility of the structural materials. A Phenomena Identification and Ranking Table (PIRT) type process as described in Regulatory Guide (RG) 1.203, "Transient and Accident Analysis Methods" (Reference 1) was used to identify significant degradation phenomena and to develop the testing and modelling qualification presented in this report.

The design of the KP-FHR does not require the application of cladding or coatings [[

]] . If coatings or cladding are used in the safety-related portions of the KP-FHR, their use in the design will be in a manner consistent with ASME Code rules. For example, ASME Section III, Division 5, Subsection HB, Subpart B for structural load carrying Class A materials (Reference 2).

This report also presents an overview of a Reliability & Integrity Management (RIM) Program for information. The RIM program is an integral part of nuclear component life management. A new approach for RIM of high temperature reactors is being developed by ASME Section XI Division 2. Article VII-4 of the Code has been reserved for molten salt reactors (and presumably solid fueled FHR designs) but has not yet been developed. A RIM program for the KP-FHR will be described as part of the licensing application of the KP-FHR.

1.1 DESIGN OF THE KP-FHR

To facilitate NRC review and approval of this report, design features considered essential to the KP-FHR technology are provided in this section. These key features are not expected to change during the ongoing detailed design work by Kairos Power and provide the basis to support the safety review. Should fundamental changes occur to these design features or revised regulations be promulgated that affect the conclusions in this report, such changes will be reconciled and addressed in future license application submittals.

1.1.1 Design Background

The KP-FHR is a U.S.-developed Generation IV advanced reactor technology. In the last decade, U.S. National Laboratories and Universities have developed conceptual Fluoride Salt-Cooled High-Temperature Reactor (FHR) designs with different fuel geometries, core configurations, heat transport systems, power cycles, and power levels. More recently, the University of California at Berkeley developed the Mark 1 pebble-bed FHR, incorporating lessons learned from the previous decade of designs

(Reference 3). Kairos Power has built on the foundation laid by Department of Energy (DOE)-sponsored, University-led Integrated Research Projects to develop the KP-FHR. Although not intended to support the findings necessary to approve this report, additional design description information is provided in the "Design Overview of the Kairos Power Fluoride Salt-Cooled, High Temperature Reactor" Technical Report (Reference 4).

1.1.2 Key Features

The KP-FHR integrates key design features and material choices into a physically compact, intrinsically safe, high temperature reactor which will be built with existing, industrially proven materials. Key design features of the KP-FHR include the use of high temperature fuel, high boiling point molten salt coolants, and low-pressure operation. This combination of the Tri-Structural Isotropic (TRISO) particle fuel, stable high boiling temperature fluoride salt coolant, and low operating stresses results in a robust reactor design with intrinsic passive safety. A comparison of the KP-FHR relative to several other reactor types is given in Figure 1, which illustrates the operating temperature range (550-650°C) and low level of irradiation exposure of metallic structural materials (<0.1 dpa for the reactor vessel [[ ]]).

The fuel in the KP-FHR is based on the TRISO high-temperature fuel. TRISO fuel is a carbon matrix coated particle fuel, originally developed for high-temperature gas-cooled reactors, in a pebble fuel element. Coatings on the particle fuel provide retention of fission products to temperatures approaching 1600°C. The primary coolant that is used in safety-related systems is a mixture of lithium fluoride (LiF) and beryllium fluoride (BeF2) salts in a ratio of approximately 2:1. This F-Li-Be based salt, i.e. 'Flibe' has been proven as an effective nuclear coolant in the Molten Salt Reactor Experiment (MSRE) program and the operation of the MSRE nuclear reactor. Furthermore, there has been significant research into the stability and compatibility of Flibe in nuclear applications since the operation of the MSRE. The KP-FHR is a low-pressure reactor which operates with a modest overpressure (~0.2 MPa or 2 atm) in the reactor vessel head space to minimize contamination of the primary coolant. The low-pressure operation and associated low operating stresses are another key design feature of the KP-FHR. Low operating stresses help enable the use of conventional metallic structural materials and provides significant margin against high temperature failure modes such as creep-rupture.

1.1.2.1 Heat Transport Systems

There are three main heat transport loops for the KP-FHR as shown in the example in Figure 2.: (1) a primary heat transport loop, (2) an intermediate heat transport loop, and (3) a power conversion loop. The primary heat transport loop utilizes pumps and piping to transfer the Flibe coolant from the reactor vessel to an intermediate heat exchanger and recirculate the Flibe back to the reactor vessel. The hot leg of the primary heat transport loop is anticipated to operate at ~650°C and the cold leg returns the Flibe to the reactor vessel at ~550°C. Note the focus of this report is on the safety-related high-temperature metallic structural components which are anticipated to be in the reactor vessel portions of the primary heat transport loop. The determination of safety-related components is performed as described in the Kairos Power Topical Report, "Risk-Informed Performance Based Licensing Basis Development Methodology" (Reference 5). [[

]] However, classification of safety-related components will be described in a future licensing submittal for a KP-FHR. If other metallic

components are considered to be safety-related in a future licensing application, Kairos Power believes that this qualification plan will provide sufficient information to provide assurance of performance.

The primary heat transport loop interfaces with an intermediate coolant loop via a heat exchanger. The intermediate heat transport systems utilize nitrate salt as the coolant [[

]] Lastly, the intermediate coolant loop interfaces with a conversion loop. The example power conversion system shown in Figure 2 is based on a conventional steam-turbine cycle that operates at high pressure and provides superheated steam to a high-pressure turbine [[ ]] Table 1 summarizes these key features and parameters of the KP-FHR.

The KP-FHR design includes two decay heat removal systems. A system for providing decay heat removal is used following normal shutdowns and anticipated operational occurrences. A separate passive decay heat removal system, the Reactor Vessel Auxiliary Cooling System (RVACS), [[ ]] removes decay heat in response to a design basis accident. Note that the RVACS does not rely on electrical power to accomplish its safety function.

1.1.2.2 Containment Approach

The KP-FHR design uses a functional containment approach, like the Modular High Temperature Gas-Cooled Reactor (MHTGR) rather than a low-leakage, pressure-retaining containment structure that is typically used for light water reactors (LWRs). The KP-FHR functional containment safety design objective is to meet 10 CFR 50.34 (10 CFR 52.79) offsite dose requirements at the plant's exclusion area boundary with margin. A functional containment is defined in RG 1.232, “Guidance for Developing Principal Design Criteria for Non-Light Water Reactors” as a "barrier, or set of barriers taken together, that effectively limit the physical transport and release of radionuclides to the environment across a full range of normal operating conditions, anticipated operational occurrences, and accident conditions. RG 1.232 includes an example design criterion for the functional containment (MHTGR Criterion 16). As also stated in RG 1.232, the NRC has reviewed the functional containment concept and found it “generally acceptable,” provided that “appropriate performance requirements and criteria” are developed. The NRC staff has developed a proposed methodology for establishing functional containment performance criteria for non-LWRs, which is presented in SECY-18-0096, “Functional Containment Performance Criteria for Non-Light-Water-Reactors”. This SECY document has been approved by the Commission.

The functional containment approach for the KP-FHR is to control radionuclides primarily at their source within the coated fuel particle under normal operations and accident conditions without requiring active design features or operator actions. The KP-FHR design relies primarily on the multiple barriers within the TRISO fuel particles and fuel pebble to ensure that the dose at the site boundary (from postulated accidents) meets regulatory limits. Additionally, in the KP-FHR (but not in MHTGR designs), the molten salt coolant serves as an additional barrier providing retention of fission products that could escape the fuel particle and fuel pebble barriers. This additional retention barrier is a key feature of the enhanced safety and reduced source term in the KP-FHR. To enable fission product retention of the Flibe coolant, the reactor vessel must retain the coolant around the fuel pebbles. Thus, the reactor vessel is considered to be a safety-related structure. [[

]]

1.1.2.3 Reactor Vessel

The anticipated design of the KP-FHR reactor vessel is based on a vertical cylinder with bottom and top heads. The vessel is expected to be constructed from materials that are qualified by the ASME Section III. The reactor vessel serves as part of the reactor coolant boundary and supports and interfaces with other systems such as rod control, pebble handling, and heat removal systems. The reactor vessel will be designed to withstand the operational loads imparted on it by the core structures, fuel, and coolant. Additionally, the reactor vessel will be of sufficient strength and resiliency to withstand off-nominal conditions required by ASME Section III Division 5 Level B, C, and D Service Conditions.

[[

]]

1.2 REGULATORY INFORMATION

1.2.1 Regulations Relevant to the KP-FHR Material Qualification

The KP-FHR is anticipated to be licensed under Title 10 of the Code of Federal Regulations (10 CFR) using a licensing pathway provided in Part 50 or Part 52. Applicants for construction permits for facilities licensed under 10 CFR 50 are required to provide a Preliminary Safety Analysis Report (PSAR), which provides a safety assessment of the facility in accordance with 10 CFR 50.34(a). Applicants for a Limited Work authorization (LWA) are required to submit a safety analysis that meets 10 CFR 50.34 for the scope of the LWA per 10 CFR 50.10(d)(3)(i). Subsections within 10 CFR 50.34(a) relevant to the requirement to describe design characteristics of the KP-FHR high temperature materials are listed below (note these are required to be updated as part of the operating license application in the Final Safety Evaluation Report (FSAR) per 10 CFR 50.34(b)(4)):

> *50.34(a)(1)(ii)(C) The extent to which the reactor incorporates unique, unusual or enhanced safety features having a significant bearing on the probability or consequences of accidental release of radioactive materials.*
>
> *50.34(a)(2) A summary description and discussion of the facility, with special attention to design and operating characteristics, unusual or novel design features, and principal safety considerations.*

Similarly, applicants for combined licenses for facilities licensed under 10 CFR 52 are required to provide a FSAR which provides a safety assessment of the facility in accordance with 10 CFR 52.79. Subsections relevant to the design and performance of high temperature materials are as follows:

> *52.79(a)(2) A description and analysis of the structures, systems, and components of the facility with emphasis upon performance requirements, the bases, with technical justification therefor, upon which these requirements have been established, and the evaluations required to show that safety functions will be accomplished. It is expected that reactors will reflect through their design, construction, and operation an extremely low probability for accidents that could result in the release of significant quantities of*

radioactive fission products. The descriptions shall be sufficient to permit understanding of the system designs and their relationship to safety evaluations. Items such as the reactor core, reactor coolant system, instrumentation and control systems, electrical systems, containment system, other engineered safety features, auxiliary and emergency systems, power conversion systems, radioactive waste handling systems, and fuel handling systems shall be discussed insofar as they are pertinent.

52.79(a)(2)(iii) The extent to which the reactor incorporates unique, unusual or enhanced safety features having a significant bearing on the probability or consequences of accidental release of radioactive materials.

Similar requirements to these are also included in 10 CFR 52.47 for Standard Design Certifications; 10 CFR 52.137 for Standard Design Approvals; and 10 CFR 52.157 for manufacturing licenses.

The use of metallic structural materials in high temperature Flibe salt environments is considered to represent a new and unique feature not typical of existing licensed light water reactor designs. The design and thermophysical properties of the KP-FHR reactor coolant enhances the safety of operations and reduces the probability of events [[

]] . The design and thermophysical properties of the KP-FHR reactor coolant also provides additional functional containment protection, beyond that provided by the TRISO fuel particle, by absorbing fission products that escape the TRISO protective layer. This design feature reduces the probability of accidental release of radioactive materials. The specification limits and thermophysical properties of the reactor coolant for the KP-FHR are provided in the Kairos Power Topical Report, "Reactor Coolant for the Kairos Power Fluoride Salt-Cooled High Temperature Reactor" (Reference 6). This report describes the qualification and testing methods for the metallic structural materials in the high temperature Flibe salt environments for use in the Flibe wetted areas containing safety-related high temperature components of the KP-FHR. As such, qualification of these materials using the methodology described in this report supports conformance, in part, to 10 CFR Part 50, Sections 50.34(a)(1)(ii)(C), 50.34(a)(2), 10 CFR 50.34(b)(4); and to 10 CFR Part 52, Sections 52.79(a)(2) and equivalent regulations in 52.47, 10 CFR 52.137, and 10 CFR 52.157.

1.2.2 Principal Design Criteria that are Relevant to the KP-FHR Material Qualification

Facilities licensed under 10 CFR Part 50 are also required to describe Principal Design Criteria (PDC) in their safety analysis reports supporting a construction permit and operating license application as described in 10 CFR 50.34(a)(3)(i). Likewise, applicants for standard design certifications, combined licenses, standard design approvals, and manufacturing licenses must include the PDC for a facility as described in 10 CFR 52.47(a)(3)(i), 10 CFR 52.79(a)(4)(i), 10 CFR 52.137(a)(3)(i), and 10 CFR 52.157(a).

The PDC for the KP-FHR have been established in the Kairos Power Topical Report, "Principal Design Criteria for the Kairos Power Fluoride Salt Cooled High Temperature Reactor" (Reference 7). The specific PDC in this report, which rely on or credit the design and performance of high temperature metallic structural materials include PDCs 14 and 31. These PDCs are discussed below.

The design and performance of high temperature metallic structural materials is relative to demonstrating conformance to PDC 14 because the materials used in the KP-FHR must ensure that they do not fail. The PDC states:

> *The safety-significant elements of the reactor coolant boundary are designed, fabricated, erected, and tested such that they have an extremely low probability of abnormal leakage, of rapidly propagating failure, and gross rupture.*

The design and performance of high temperature metallic structural materials is relative to demonstrating conformance to PDC 31 because the materials used in the KP-FHR must ensure that they are not unduly stressed under operating, maintenance, testing, and postulated accidents. PDC 31 states:

> *The safety significant elements of the reactor coolant boundary are designed with sufficient margin to ensure that when stressed under operating, maintenance, testing, and postulated accident conditions, (1) the boundary behaves in a nonbrittle manner and (2) the probability of rapidly propagating fracture is minimized. The design reflects consideration of service temperatures, service degradation of material properties, creep, fatigue, and other conditions of the boundary material under operating, maintenance, testing, and postulated accident conditions, and the uncertainties in determining: (1) material properties, (2) the effects of irradiation and coolant composition, including contaminants and reaction products, on material properties, (3) residual, steady-state, and transient stresses, and (4) size of flaws.*

Corrosion of structural materials is an important consideration for maintaining the integrity of the safety-significant portions of the reactor coolant boundary. Demonstration, through qualification, of the acceptability of the metallic structural materials used in the safety-significant portions of the reactor coolant boundary is a key element in establishing conformance to PDC 14 and PDC 31. The qualification requirements described in Section 2 of this report, partially satisfy PDC 14 and PDC 31. A description of how the remaining portions of these PDC are satisfied will be provided in safety analysis reports submitted with licensing applications for the KP-FHR.

1.2.3 Regulatory Request

Kairos Power is requesting NRC approval of the metallic materials qualification methodology described in Section 2 of this Topical Report for use by applicants for licenses of a KP-FHR under 10 CFR Part 50 and 10 CFR Part 52, and expects that, when the acceptance criteria for the qualification items in Tables 3-12 are met, the metallic materials described in this report (316H base metal and 16-8-2 weld filler metal) are qualified for use in the KP-FHR and support conformance, in part, to PDC 14 and PDC 31; and the requirements to describe new and novel features required by 10 CFR Part 50, Paragraphs 50.34(a)(1)(ii)(C), 50.34(a)(2), 50.34(b)(4); and to 10 CFR Part 52, Sections 52.79(a)(2) and equivalent regulations in Sections 52.47, 52.137, and 52.157.

2 STRUCTURAL ALLOYS

2.1 BACKGROUND

Ductile, face-centered-cubic iron and nickel-based alloys (i.e. 'austenitic' alloys) are commonly used structural materials in light water reactors due to their combination of strength, toughness, and corrosion-resistance. Light water reactor operation involves modest temperatures (215-345°C) but relatively high operating pressures (~7 MPa for BWR's and 16 MPa for PWR's). These temperatures translate into homologous temperatures (TH)1 of ~0.27-0.36 for the structural materials. These homologous temperatures are low enough such that solid state diffusion rates are slow and many degradation phenomena (e.g., alloy phase stability, creep, etc.) are of limited consequence.

Like LWR's, the KP-FHR design intends to use iron and nickel-based alloys for metallic structural components but at much higher temperatures, lower pressure, and in different coolant chemistry environments than light water reactors. Specifically, the design of safety-significant components of the KP-FHR will use austenitic alloys at homologous temperatures [[ ]] in both reducing and oxidizing molten salts. These higher temperatures require more consideration of high temperature material phenomena (e.g., creep deformation) and, like water reactors, the molten salt coolants will require compositional control to ensure the metallic structural materials maintain resistance to corrosion and to environmentally assisted cracking. For comparison, the approximate operating pressures and temperatures of LWR's, high temperature gas reactors HTGR's and sodium-cooled fast reactors (SFR's) and the KP-FHR is given in Figure 3. As shown, the KP-FHR will operate at significantly lower pressures than the BWR's, PWR's and high temperature gas reactors and at comparable pressures but somewhat higher temperatures than SFR's.

2.2 STRUCTURAL ALLOY SELECTION

The design of the KP-FHR reactor coolant boundary will be constructed from alloys qualified (or near qualification) by the ASME Code. Currently in ASME, Section III, Division 5, there are only a few alloys that are suitable for temperatures ≥ 600°C. These include the austenitic Alloys 304H, 316H, 800H, and 617. Additionally, a modified version of Hastelloy N, the DOE developed Alloy 709, and the stainless-steel weld filler metal ER16-8-2 were included in the consideration for structural alloy selection. These 7 alloys were ranked based on ten criteria:

- Status of ASME Section III Code Qualification
- Mechanical & Physical Properties
- Experience with Molten Salts
- Experience in Nuclear Reactor Systems
- Technical Maturity
- Ability to Procure the Alloy in a Wide Variety of Product Forms
- Ease of Fabrication and Existence of a Matching Weld Filler Metal
- Environmental Compatibility of the Alloy with the KP-FHR Environments
- Degree of Regulatory Acceptance of the Alloy for use in Nuclear Systems
- Cost of the Alloy

[1] Homologous temperature is defined as the temperature of interest divided by the melting point of the pure element that that alloy is based on in absolute units.

The results of these rankings are given in Table 2. In Table 2, the ranking for each category were assigned on a scale of 1 to 5 with a high rank (1 or a blue filled circle) being the most desirable and a low rank (5 or an open circle) being the least desirable. A brief summary of the factors that influenced eliminating the other structural alloys are given below.

Alloy 304H is similar to Alloy 316H in composition and in many attributes. However, 304H displays notably lower strength at high temperatures. The benefits of 304H relative to 316H are few (e.g., marginally lower cost) and do not provide compelling reasons to select this alloy over 316H. For these reasons, 304H was eliminated from consideration in favor of the more capable 316H.

Alloy 800H is less creep-resistant than 316H and contains higher levels of chromium (~21 wt.% Cr vs. ~17 wt.%). Furthermore, 800H does not have a matching weld filler metal but is often welded with high chromium nickel-based alloys such as EN82H. Higher chromium levels are undesirable for corrosion-resistance in Flibe and the increased nickel in 800H/EN82 relative to 316H/ER16-8-2 is less desirable due to the potential transmutation of nickel to helium, which will adversely affect irradiation embrittlement. For these reasons, 800H is ranked lower than 316H stainless steel.

Alloy 617 possesses superior high temperature strength and creep resistance relative to 316H. However, the alloy contains a large amount of cobalt (10-15 wt.%) which undergoes undesirable neutron activation. The high strength of 617, while desirable, is not required for the KP-FHR design. Moreover, the attractive high temperature strength can present challenges when trying to hot-form the alloy and lead to fabrication challenges. Lastly, due to the expense and limited market for 617 relative to more common alloys like 304 and 316, 617 is only commercially available in limited product forms.

Hastelloy N showed excellent corrosion-resistance in the MSRE experience but was susceptible to both tellurium embrittlement and degradation by irradiation (Reference 8 and 9). For this reason, a modified grade of Hastelloy N was considered in the rankings. However, Hastelloy N is not currently approved for use by ASME Section III for high temperature reactors and modified grades are likely different enough in composition (e.g., containing several weight % of niobium) to require a full ASME qualification effort. Furthermore, a suitable weld filler metal for a modified Hastelloy N was not readily apparent. The absence of existing ASME Section III code qualification, commercialization, and high costs associated with bringing a new alloy to market are major limitations that precluded selecting a modified grade of Hastelloy N.

Alloy 709 is an advanced stainless steel being developed by the DOE for nuclear power applications. While not ASME Section III qualified, this effort is in progress and to date, Alloy 709 displays a desirable combination of properties with higher creep strength than Alloy 316H as well as the potential for increased resistance to irradiation damage via alloy design. Notably, welding of Alloy 709 with a weld filler metal of the same composition indicates promising properties with weld degradation factors near 1. While the lack of current ASME Section III code qualification and industrial supply lowers the current ranking of this alloy, it may be considered for use in future licensing applications for the KP-FHR.

Alloy 316H and its weld filler metal ER16-8-2 possess a desirable combination of properties relative to the other candidate alloys. Alloy 316H is currently ASME Section III qualified, exhibits desirable mechanical properties, has demonstrated compatibility with Flibe salt, and has an extensive experience base in nuclear reactor applications. Furthermore, the alloy is technically mature with good availability, fabricability, and relatively low cost. The weld filler metal ER16-8-2 indicates notable creep resistance and

a high degree of weldability with 316H. Areas that require additional work for this alloy include extending the qualification of ER16-8-2 to higher temperatures (currently in the ASME Section III code, the filler metal is limited to 650°C in the 2017 ASME Section III code), and additional research into the corrosion and environmental compatibility of these materials in Flibe. Based on this review, 316H/ER16-8-2 were selected as the metallic structural materials for safety-related components in the KP-FHR. These alloys were used as the basis for the expert panel PIRT review described in Section 2.5.1 which assessed environmental compatibility in Flibe salt. The remainder of the report is limited to the use and qualification of 316H / ER16-8-2 for safety-significant components in Flibe wetted areas of the KP-FHR.

2.3 INDUSTRIAL EXPERIENCE WITH ALLOY 316H AND ITS WELD FILLER METALS

The following sections briefly describe the use of Alloy 316 in conventional nuclear reactors, advanced nuclear reactors, in non-nuclear but comparable industrial applications, and its compatibility with molten salt.

2.3.1 Conventional Nuclear Reactors

Austenitic stainless steels including type Alloy 316 stainless steel and its closely related variant Alloy 304, along with their weld filler metals, are commonly used for light water reactor internal components and corrosion-resistant cladding. Components made from these steels include fuel support structures, core barrels, flow baffle plates, and reactor vessel cladding. The low carbon variant of the alloy (i.e., the 'L' grade) is commonly used since high temperature strength is not limiting, but grain boundary chromium depletion (i.e., sensitization) is a concern. In light water reactors, grain boundary sensitization can result in intergranular corrosion and intergranular stress corrosion cracking if coolant chemistry is not maintained (e.g., if there is significant oxygen present in the coolant). However, sensitization is not detrimental to corrosion in Flibe. Flibe salt is highly reducing and corrosion-resistance does not rely on the formation of a passive oxide film but on metallic stability in the salt. For stainless steels exposed to Flibe, the primary corrosion mechanism has been established as chromium loss (usually via grain boundary diffusion) to the coolant (Reference 10 and 11). Thus, sensitized microstructures can be beneficial since lower chromium at the grain boundary results in less chromium lost via grain boundary diffusion.

2.3.2 Advanced Nuclear Reactors

Austenitic stainless steels, including Alloy 316 have seen extensive experience in Sodium-Cooled Fast Reactors (SFRs) (Reference 12 and 13). In SFR's, austenitic stainless steels have been used throughout the primary plant with good experience. Analogous to corrosion in molten salt, when impurities in sodium such as oxygen and hydrogen are controlled to low levels, corrosion rates are low and are governed by alloying element solubility levels in the coolant (Reference 14).

While the nickel- based alloy Hastelloy N was chosen as the structural alloy for the MSRE construction, Alloy 304 and Alloy 316 were assessed in the MSRE program for their resistance to corrosion and to tellurium embrittlement (Reference 15, 16, and 17). In loop-type corrosion tests (i.e., tests with a hot leg and a cold leg) using Flibe salt at 650°C, these austenitic stainless steels exhibited corrosion rates ≤ 25 µm/year for short exposure times (<3000 hours) which decreased with time to ~8 µm/year after 3000-9000 hours exposure (Reference 16 and 17). Furthermore, when redox control of the salt was implemented (using Be metal additions), corrosion rates at 650°C were further reduced to levels

estimated as <2 µm/year (Reference 16). While graphite can be a factor which increases corrosion rates, the data of Zheng et al., indicate this is a relatively modest ~2X increase in corrosion rate (Reference 18).

These results indicate that corrosion will be manageable for Alloy 316 components in the KP-FHR. For example, consider a thin walled component such as a heat exchanger tube [[ ]] . Taking a reasonable, if not conservative corrosion rate of 2 microns per year (recall, Keiser et al., showed <2 µm/year (Reference 16) for Alloy 316 at 650°C in redox controlled Flibe) for a [[ ]] lifetime produces chromium loss to a depth of 0.04 mm (0.0016") or < 4% of the wall thickness. It is important to note that this 0.04 mm represents a degraded layer (Cr loss), not a true reduction in wall thickness. In the chromium depleted layer, ~82% of the alloy remains (i.e., Alloy 316 is ~18 atomic % Cr).

In addition to manageable corrosion rates in Flibe salt, austenitic stainless steels also exhibit greater resistance to tellurium embrittlement (Reference 19 and 20). The mechanism of tellurium embrittlement is well understood to be a result of the nickel – tellurium intermetallic formation (Reference 15, 21, 22, 23, and 24). Given the much lower nickel content of Alloy 316 compared to Hastelloy N, this intermetallic formation is less likely and a lower risk (Reference 25). Moreover, the KP-FHR design mitigates concern for tellurium embrittlement by the use of solid fuel and redox control of the salt (Reference 6). With the very low TRISO particle failure rate demonstrated in the DOE Advanced Gas Reactor program combined with the retention of tellurium in the fuel particle (Reference 26), the concentration of tellurium in the Flibe is expected to significantly lower than the liquid fueled MSRE. Furthermore, the [[ ]] redox control moves the electrochemical potential of the system away from the oxidizing regime of concern (Reference 6 and 15). For these reasons, concern for tellurium embrittlement in the KP-FHR are minimal.

2.3.3 Other Industrial Applications of Alloy 316

Austenitic stainless steels, including type Alloy 316H are used in a wide variety of high temperature industrial applications due to their corrosion-resistance, generally desirable mechanical properties, and wide industrial availability of product forms (Reference 27). For example, Alloy 316H, its welds, and similar austenitic stainless steels (Alloy 347 and Alloy 321) are used extensively in oil and gas refinery applications at temperatures and time frames of relevance to the KP-FHR (Reference 28 and 29). For example, petroleum refining applications of stainless steels include crude distillation, fluid catalytic cracking, delayed coking, hydrotreating, catalytic reforming, hydrocracking, gas plant, amine plant, sulfuric acid alkylation, and sour water stripper systems.

Furthermore, Alloy 316H and its weld metals are used in other industries near the time and temperature of the KP-FHR. Figure 4 illustrates the intended operation of the KP-FHR in the blue box ([[ ]] at 550°C-650°C), relative to the NIMS creep database (gray box) and selected high temperature, long life oil and gas refinery (FCCU and Cyclone) components; the typical operating temperatures and service life of these components is estimated from (Reference 29). As shown, the KP-FHR is designed to operate at somewhat lower temperature and longer times than components in the oil and gas industry. However, it is important to note that (1) there is overlap in the time/temperature ranges of experience and (2) many oil and gas components operate at higher stresses and are limited by different environmental degradation phenomena than those of the KP-FHR. For example, Fluid Catalytic Cracking Units are typically exposed

severely carburizing gaseous environments that can limit component life and rapid temperature cycles which generate appreciable thermal stresses (Reference 29). Neither condition is pertinent to the KP-FHR.

2.3.4 Compatibility with Molten Salts

In reducing salts, Alloy 316 is used in the pyro-processing of spent nuclear fuels. In that technology, chloride-based salts are used to convert oxide based nuclear fuel back to their metallic form (Reference 30, 31, and 32). In pyro-processing systems, austenitic stainless steels are used as structural alloys and generally display excellent corrosion-resistance as long as the salt is relatively free from oxidizing impurities (Reference 33).

With respect to the reducing salt of interest to the KP-FHR (Flibe), there are significant laboratory data to support the use of Alloy 316 as a structural alloy. Corrosion data for Alloy 316 exposed to Flibe and (Flibe + fuel) are summarized in Figure 5 (Reference 16, 17, 18, and 34). As shown, the data exhibits an apparent activation energy ~56 kJ/mol. Corrosion rates of Alloy 316 in the temperature range of interest for normal operation (550-650°C) are on the order of 5-30 µm/year. Based on the data of Keiser as well as other literature work, redox control of the salt potential can further decrease corrosion rates to < 2 µm/year (Reference 16). Also shown on the plot is the effect of coupling to graphite on the corrosion rate. Zheng et al., performed 1:1 experiments with and without graphite and showed about a 2 times increase in corrosion rate with graphite (Reference 18). This effect of graphite is confirmed by more recent work on 316 in FLiNaK salt (Reference 35). In the FLiNaK research, the graphite to stainless steel area was varied and again, an acceleration of approximately 2X was found with the largest graphite / stainless steel area of 3:1 (Reference 35). Also, of note are the data of Koger, which are for Flibe + fuel (ThF4+UF4) (Reference 17). That sample showed slightly higher corrosion rates but appear very similar to the pure Flibe data (Reference 36).

2.4 EXTENSION OF ASME CODE STRESS RUPTURE FACTORS FOR ER16-8-2 FILLER METAL

2.4.1 Material Property Gaps

As mentioned in Section 2.1, ER16-8-2 weld filler metal is currently qualified up to 650°C in the ASME Section III code while Alloy 316H is qualified to 816°C (Reference 37). The KP-FHR reactor vessel is anticipated to operate at ~550°C during nominal operations but could experience temperatures up to [[ ]] for short durations during infrequent incidents or abnormal operating occurrences. Thus, an extension of the ASME Section III code qualification for ER16-8-2 up to [[ ]] . Mechanical testing of weldments will be required as described in the following paragraphs to develop a Code Case introducing stress rupture factors for Alloy 316 weldments with ER16-8-2 filler metal for temperatures between 650°C and [[ ]] .

2.4.2 Testing Required to Develop ASME Code Case

The types of mechanical testing that are necessary to develop a Code Case for extending the stress rupture factors for Alloy 316 weldments with ER16-8-2 filler metal are described in ASME Section III Division 5, Non-Mandatory Appendix Y (Reference 38). The methods of testing that are required for such weldments as specified in Appendix Y are the ASTM E21 Elevated Temperature Tensile Testing, ASTM E2714 Creep-Fatigue Testing, and ASTM E139 Creep-Rupture Testing.

2.4.2.1 Elevated Temperature Tensile Testing

Elevated Temperature Tensile Testing will be performed per ASTM E21 on all-weld-metal and cross-weld specimens at temperatures between 650°C and [[ ]] (1200°F – [[ ]]) at intervals of 38°C (100°F). These tests will determine the 0.2% yield strength, ultimate tensile strength, % elongation and % reduction in area at each temperature. Additionally, the strength of the ER16-8-2 all-weld-metal at each temperature will be used to establish the creep-rupture and creep-fatigue test stresses.

2.4.2.2 Creep-Fatigue Testing

Nonmandatory Appendix HBB-T of Section III, Division 5 provides a means to assess creep-fatigue of base metals, but it does not provide a dedicated means to assess creep-fatigue of weldments (Reference 37). Instead, the creep-fatigue analysis for base metals is applied to areas with welds and conservative restrictions are applied as follows (see HBB-Y-3400 of Reference 37);

> *"(a) limiting the inelastic accumulated strains to one-half the allowable strain limits for the base metal*
>
> *(b) limiting the allowable fatigue at weldments to one-half the design cycles allowed for the base metal*
>
> *(c) reducing the allowable creep rupture strength at weldments to a fraction of the base metal value through the weld strength rupture factor when determining time-to-rupture."*

Creep-Fatigue testing per ASTM E2714 of all-weld-metal and of cross-weld specimens is performed only to verify the adequacy of the HBB-T treatment of weldments (Reference 38). If the restrictions specified in HBB-Y-3400 bound the ASTM E2714 creep-fatigue test data, then the Non-mandatory Appendix HBB-T analysis procedures for base metal with specified restrictions for welds will have been determined to be adequate for creep-fatigue analysis of welds.

2.4.2.3 Creep-Rupture Testing

Creep-Rupture tests will be performed in accordance with ASTM E139 (Reference 39). The time, temperature and load conditions for the creep-rupture tests are derived from design Service Level conditions. ASME Section III Division 5 HBB-Y-2200 allows creep-rupture curves to be extrapolated up to a factor of five from the maximum creep-rupture test duration. The maximum operating service time at each temperature is therefore divided to determine the minimum required-creep test duration. For example, for a 100,000-hour service lifetime at a given temperature, a minimum test duration of 20,000 hours is sufficient to bound the operating life. The test duration and temperature can then be inserted into the appropriate creep correlation (e.g. the Larson-Miller model) to estimate the test load that will be required to produce specimen rupture at each specified time and temperature combination (Reference 40). Metallurgical analysis will be performed on failed specimens to support extrapolations beyond a factor of three in accordance with HBB-Y-2200.

Testing will be performed on both all-weld-metal ER16-8-2 specimens as well as on cross-weld specimens. The rupture strength of the weld metal will be divided by the rupture strength of the base metal at each time and temperature combination to determine proposed stress rupture factors.

After completion of the above testing, an ASME Code balloting plan will be developed and the proposed rupture factors and supporting data will be presented to the relevant ASME Code Committees for review and approval. Progress on this extension is presently being tracked through ASME Codes & Standards Record #19-2745. Once the Code Case has been approved by ASME, then it will be presented to the NRC for approval. Once approved by the NRC then the stress rupture factors at the higher temperatures will be used in the same manner as those at the lower temperatures to determine the allowable stresses for specific temperature and time durations.

2.5 DEMONSTRATION OF ENVIRONMENTAL AND IRRADIATION COMPATIBILITY

As noted above, Alloy 316H is already an acceptable material for use in high temperature reactor applications in ASME Section III. However, the code requires demonstration of the environmental and irradiation compatibility of the structural materials. For the KP-FHR safety-related systems, the environments of interest include high temperature air (external to the system) and molten Flibe salt (internal to the system), with exposure to neutron irradiation.

2.5.1 Review of Environmental and Irradiation Compatibility Issues

Due to the breadth and complexity of environmental issues, an expert panel was convened to assess potential environmental issues for Alloy 316H / ER16-8-2 in each of the KP-FHR heat transport loops. This review utilized a process based on the Phenomena Identification and Ranking Table (PIRT) methodology in NRC Regulatory Guide 1.203. Only the environmental degradation issues pertinent to potential safety-related components (exposed to Flibe and air) are summarized in this report. Component materials degradation considerations are summarized in Figure 6, which presents the Venn Diagram for the Material – Stress/Strain – Environment degradation phenomena of concern. that the expert panel consisted of experts from national laboratories, universities, and consultants.

In total, there were 23 degradation phenomena assessed by the expert panel in 7 unique systems, structures, and components (SSC's). This resulted in 198 scenarios assessed by the expert panel to start, with ten scenarios added during the PIRT for 208 total rankings. Each scenario was ranked based on its importance (high, medium, low) and the degree of knowledge (high, medium, low). The PIRT rankings are shown schematically in Figure 7. Phenomena with high importance and low knowledge are the greatest priority (upper right box), followed by phenomena with high importance and medium knowledge (upper center box) and phenomena with medium importance but low knowledge (middle right box). These categories are given a numerical ranking, where Category #1 indicates that highest priority phenomena to investigate (high importance and low knowledge), Category #2 is the next important, etc. Note that each degradation phenomenon was ranked so that a total of seven, equally weighted rankings were used to develop average knowledge and importance levels.

In considering the results of the review, a conservative approach was adopted to determine which phenomena warranted future investigation. Rather than take an average ranking, phenomena were considered based on if any Expert gave it a ranking of 1 (High Importance / Low Knowledge), 2 (High Importance / Medium Knowledge), or 3 (Medium Importance / Low Knowledge). Results from those rankings are given in Figure 8. The excluded phenomena are of such low importance or high knowledge as to not warrant further consideration.

In Figure 8 the open symbols identify phenomena that will be addressed by further investigation while the 'X' symbols show the low ranking of the phenomena that will not be addressed. The degradation concerns that warrant further investigation are grouped into categories with corrosion related phenomena being identified by blue circles, environmentally assisted cracking by green squares, 'other' phenomena by gray triangles and irradiation effects by red diamonds.

The resulting phenomena to be further addressed are presented in Table 4, which summarizes the issues. Note that Table 4 only presents the degradation phenomena for safety-related components. The degradation phenomena are grouped into four categories: corrosion, environmentally assisted cracking, 'other' phenomena, and irradiation effects. For each category, the phenomenon of interest is listed along with a brief description and major variables that additional investigation will address.

2.5.2 Research to Address Environmental Compatibility

Three non-irradiated materials testing categories were identified in Table 4 (Corrosion, Environmentally Assisted cracking, and Other Phenomena) that require additional investigation. The following sections describe the testing and modelling that will address those areas with respect to metallic structural material qualification. The result of these efforts is to establish the appropriate design, operation, and inspection requirements for [[ ]] of the metallic structural materials in the safety-significant components of the KP-FHR. Unless otherwise noted, all tests will be performed on the base materials (Alloy 316H) and on the weld filler metal (ER16-8-2). Additional investigation activities to address irradiation effects is described in Section 2.5.3.

In addition to the data that will be generated through the qualification program for 316H and 16-8-2 described in this report, Kairos Power also intends to review the open literature for relevant data. If applicable to the current testing programs, literature data may be used to help validate or extend the data and models resulting from the present testing program.

Testing related to safety-related components will be conducted under a 10 CFR 50 Appendix B NQA Testing Program. Testing associated with non-safety related special treatment components is consistent with NRC guidance provided in Standard Review Plan 17.5, Quality Assurance Program Description – Design Certification, Early Site Permit and New License Applicants. This information is provided in the Kairos Power Topical Report, "Quality Assurance Program for the Kairos Power Fluoride Salt-Cooled High Temperature Reactor Topical Report (Reference 41).

2.5.2.1 Flibe Composition and Monitoring via Electrochemical Potential

For testing in Flibe (e.g. corrosion tests and environmentally assisted cracking (EAC) testing), two basic conditions will be explored: (1) 'nominal Flibe' i.e. Flibe which has been purified to minimize water and other oxidizing contaminants but not with [[ ]] (Reference 6) and (2) tests which intentionally add a reducing agent [[ ]] to lower the electrochemical potential of metal samples in the salt. Note that the starting Flibe salt in each case shall meet or exceed the compositional guidelines outlined in Reference 6. In this manner, Kairos Power can obtain meaningful corrosion rate and EAC data in the more aggressive 'nominal Flibe' salt and assess the expected benefit of operating at the less aggressive condition of redox control.

Electrochemical potential (ECP) monitoring will be the primary method used to assess the condition of the salt, monitor for ingress of oxidizing agents (air), and to help rationalize the data from different testing runs. Additionally, compositional analysis of the salt pre- and post- test will be also be used to understand and document the effects of corrosion products on corrosion and EAC testing. Separate research, which is outside of the scope of this report, will be used to determine the targeted electrochemical potential ranges for both nominal (high ECP) and reduced Flibe (low ECP).

2.5.2.2 Corrosion Testing & Modelling

Corrosion testing of prototypical materials will be conducted in order to develop quantitative corrosion rate models for Alloy 316H and on the weld filler metal ER16-8-2 in Flibe. Corrosion testing will utilize unstressed coupons of Alloy 316H and ER16-8-2 weld filler metal in representative conditions as shown in Table 5. The majority of the testing will be conducted in "nominal Flibe", i.e. Flibe which has been purified to minimize water and other oxidizing contaminants but not with [[

]] (Reference 6). In this manner, meaningful corrosion rate data can be obtained with test durations up to 10,000 hours. Corrosion testing will be conducted under nominal conditions consistent with the anticipated flow, exposure to graphite, and thermal conditions (i.e. systems with both hot and cold legs) of the KP-FHR. In addition, selected testing may also be performed in off-nominal conditions in order to account for the effects of impurities on the nominal corrosion behavior. For example, static salt pots may be used to conduct experiments to assess impurity effects.

The planned corrosion testing is summarized in Table 5 which gives the purpose of the test, the materials to be tested, the environment and the approximate test temperatures and duration. For each test, the depth of chromium loss will be assessed over time to establish the governing corrosion kinetics (Equation 1) and to establish the steady state corrosion rate. Note that while the weight change of each corrosion coupon shall be documented, Kairos Power intends to use analytical electron microscopy to determine the extent of corrosion or other metallurgical changes (e.g. Cr loss depth, carbide precipitation, etc.). Additional details of the corrosion testing and an example of the planned statistical analysis of the data are provided in Appendix C. More detailed descriptions of the rotating cage loop (RCL) and in-situ mechanical (ISM) test systems are given in Appendix D.

The purpose of each test is further elaborated below. For most tests, the corrosion rate will be established by assessing the depth of chromium loss from the sample surface. The chromium loss depth will be determined by an appropriate analytical technique such as wavelength dispersive spectroscopy. In addition, the weight change of the corrosion coupons will be determined. The following bullets expand on the purpose of each test.

$$Cr\ loss\ depth \propto \left(t, \sqrt{t}, log\ t, \frac{1}{log\ t} etc.\right) \qquad \text{Eq. 1}$$

- Temperature: The testing as a function of temperature in nominal Flibe for Alloy 316H and ER16-8-2 will determine the corrosion rate for each alloy and will be used as a baseline to judge subsequent separate effects testing. At each of the three planned temperatures, tests will be conducted for different times to determine the controlling kinetics and the steady state corrosion rate. The steady state rates will then be used to develop best-estimate and design-estimate predictions of corrosion rate as a function of temperature. These data will be fit to a model of the

form of Equation 2 and provide a standard against which the separate effects tests described below can be quantitatively judged.

$$Corrosion\ Rate = f(Alloy, t, T, ECP, Condition, etc.) \qquad \text{Eq. 2}$$

- Microstructural Effects: The effects of the weld heat affected zone, post-weld-heat-treatment, thermal aging, and cold work will be assessed and compared to the baseline (temperature dependent models).

- Salt Composition: The salt composition testing will assess the effects of the impurities and redox control. The impurity testing will cover hypothetical accident scenarios defined in the materials PIRT review: nitrate ingress for 168 hours and air ingress for 168 hours (i.e., scenarios 3 and 4). The conditions of the accident scenarios have not been defined at this time and will be provided in safety analysis reports submitted with a future license application. These tests will determine the effect of potential loss of salt chemistry control on the corrosion rate. Redox control will be investigated via separate effects testing in order to define a factor of improvement in corrosion rate relative to the nominal Flibe purity.

- Occluded Geometry: The intent of these tests is to investigate if a physical crevice influences the corrosion rate with and without redox control of the salt.

- Erosion-Corrosion: These tests will assess the potential effect of erosion-corrosion. Specifically, graphite particulate will be introduced into corrosion tests with flow to assess if hard particles (e.g. potentially from the graphite reflector) will significantly impact corrosion rates. In these tests, weight change of the coupon (vice chromium loss depth) will be used as the primary indicator of the corrosion rate.

- Cold Leg Occlusion: In addition to the effect of temperature on the corrosion rate (hot leg samples), many of these tests described above will be used to assess the potential for cold leg occlusion. In that work, a combination of testing and modelling will be performed to determine the amount of corrosion product that is dissolved in the hot leg and precipitates out in the cold leg. Furthermore, the corrosion test system cold legs will be inspected to compare predicted vs. observed corrosion product deposition.

2.5.2.3 Environmentally Assisted Cracking

Literature data for environmental degradation of both stressed and unstressed samples were recently reviewed in Reference 42. In general, there has been little mechanical testing in molten salts and few data of relevance to the KP-FHR. In part, this is due to the difficulty of conducting in-situ mechanical testing in highly reducing molten salt. An in-situ mechanical testing system was developed to support additional investigation of this phenomena which is shown schematically in Figure 9. Key features of the testing systems include:
[[

]]

The in-situ mechanical testing systems will be used to conduct the slow strain rate, corrosion fatigue, stress corrosion cracking, and in-situ creep testing described below.

2.5.2.3.1 Slow Strain Rate Testing

Slow strain rate testing (SSRT) will be conducted in nominal Flibe to assess if Alloy 316H and ER16-8-2 are susceptible to environmentally assisted cracking in fluoride salts. The SSRT is a well-established and accepted methodology to determine susceptibility to stress corrosion initiation and crack growth (Reference 43). Testing will be conducted in accordance with ASTM guidelines outlined in ASTM G129-00 (Reference 44). The SSRT tests will be conducted on flat, pin-loaded specimens. Tests will be conducted at three different temperatures 550, 600, and 650°C, at strain rates between $1x10^{-6}$ - $5x10^{-8}$ (in/in)/sec. In the tests, the degree of an environmental effect will be assessed by comparison of the load/stroke curves with identical tests conducted in air as shown schematically in Figure 10.

2.5.2.3.2 Fracture Mechanics Based Testing: Corrosion Fatigue and Stress Corrosion Cracking

In addition to the slow strain rate testing, fracture mechanics-based testing will be performed on pre-cracked samples based on established methods (Reference 45). These tests will assess prototypical materials (Alloy 316H and ER16-8-2 weld filler metal) and be conducted in nominal Flibe at 550, 600, and 650°C. These tests will include both a corrosion fatigue portion of the test and a constant stress intensity factor portion of the test to address stress corrosion cracking. The corrosion fatigue portion of the test will initially be at relatively high ΔK's to produce fatigue crack growth and will subsequently shed load to both (1) determine the 'Stage II' Paris-law crack growth rate and (2) to prepare the sample for subsequent stress corrosion cracking testing. These in-salt fatigue crack growth rates will be compared to similar data determined at temperature but in-air to assess any potential degradation, e.g. the difference between in-air vs. in-salt behavior. Example corrosion fatigue data and their comparison to air data are shown in Figure 11. At the completion of the corrosion fatigue portion of the testing, constant stress intensity factor (KI) testing will be conducted. The intent of these tests is to trigger stress corrosion cracking under aggressive testing conditions and then transition to conditions that are more representative of the KP-FHR. One potential SCC mechanism (strain accelerated corrosion and subsequent intergranular cracking) is shown schematically in Figure 12.

2.5.2.3.3 Environmental Creep Testing

Creep-rupture testing in Flibe will be conducted to further assess the compatibility of Alloy 316H and ER16-8-2 filler metal with the molten salt. This testing will target creep rupture times on the order of 500 hours and 2000 hours. The creep tests will be conducted at 550°C and 650°C in redox controlled Flibe and will assess the integrated effects of environment and stress on the materials performance. These creep rupture times will be compared to data from air tests and the samples will be characterized for chromium loss and compared to unstressed corrosion coupons. The targeted environmental creep test conditions are given in Table 8.

2.5.2.4 'Other' Phenomena

The potential environmental degradation phenomena grouped into the 'other' category were stress relaxation cracking, phase formation embrittlement, and degradation driven by thermal cycling or by thermal gradients. Each of these phenomena will be addressed to assess the risks of each phenomenon for Alloy 316H.

To address stress relaxation cracking of Alloy 316H, stress-rupture tests will be conducted on notched bars to assess the effect of triaxial stress on cracking susceptibility per the methodology developed by Spindler (Reference 46). Tests will be conducted to compare the susceptibility of Alloy 316H to Alloy 347 stainless steel (which is notably susceptible to this type of cracking) and to assess the effect of a post-weld heat treatment. For example, Spindler et al., have noted that a 750°C / 1 hr post-weld heat treatment can provide significant resistant to stress relaxation cracking in Alloy 316H (Reference 47). The data will be used to better assess the risk of stress relaxation cracking in KP-FHR components and to develop strategies (e.g. heat treatment and design changes) to mitigate this concern.

Testing for phase formation embrittlement addresses the concern that some element could be picked up by the stainless-steel during exposure to Flibe (e.g. carbon or beryllium) and form a deleterious second phase. For example, near-surface carbide precipitation in Alloy 316 exposed to Flibe+ graphite has been noted by Zheng et al. (Reference 18). Similarly, when beryllium metal is coupled to nickel, iron, or stainless steel and exposed to elevated temperature, Be diffuses into the other metal and can exacerbate corrosion rates (Reference 48). When excess Be is present in nickel, iron or similar alloys, Ni-Be precipitates can form and increase corrosion rates, possibly by generating internal stress (Reference 48 and 49). [[

]] These samples will include at least one SSRT sample and one in-situ creep sample as detailed in Table 10.

Lastly, degradation of materials can be driven by thermal phenomena that are influenced by the environment. For example, poor mixing in the coolant could lead to local temperature gradients and result in unwanted thermal stresses (thermal striping). Similarly, the large thermal transients associated with draining and/or filling the reactor vessel could result in 'ratcheting' of the pressure vessel. However, several design features and the high Prandtl number of Flibe act to reduce the magnitude of thermal stresses (Reference 50). These phenomena are considered to be appropriately addressed via analysis and specific concerns can be mitigated via design and operational procedures without the need for testing.

Specifically, the packed bed geometry configuration of the KP-FHR allows for lateral thermal dispersion along the length of the active core while the random packing of the fuel pebbles promote thermal mixing which reduces the temperature gradients present on solid structures. Additionally, Flibe possesses relatively low thermal conductivity (~1.0 W/m-K) and high Prandtl number (~18.5) inhibit heat transfer from the coolant to solid structures as compared to liquid sodium systems which have a high thermal conductivity (60 -80 W/m-K) and very low Prandtl numbers (~0.005). This is exhibited in the very high convective heat transfer coefficients for sodium systems in comparison to convection coefficients for the Flibe KP-FHR operating range. While thermal gradients can exist in the molten salt, the poor fluid to solid structure convective heat transfer attenuates the temperature gradients reducing the risk of thermal

striping cycle fatigue. Kairos Power will rely on CFD simulation results, and, more specifically, temperature distributions at metal/salt interfaces in order to accurately capture the material's mechanical response, including thermal cyclic strains induced by variations of the Flibe temperature. In the case of safety-related components, (thermal) fatigue damage will be assessed as per ASME Section III Division 5 and (while benefiting from the KP-FHR core design and the attributes of Flibe) engineered to remain compliant with Code's allowable limits.

2.5.3 Additional Investigation to Address Degradation from Irradiation

The PIRT review identified three irradiation-influenced phenomena that may warrant additional work; irradiation-induced embrittlement, irradiation affected corrosion, and irradiation assisted stress corrosion cracking (IASCC). The following sections describe the additional investigation activities to address irradiation effects. The results of these efforts are to establish the appropriate design, operation, and inspection requirements for the [[ ]] of the metallic structural materials in the safety-significant portions of the KP-FHR, exposed to high radiation fields, [[ ]] . The estimated evolution of dpa and He in the reactor vessel over its lifetime is shown in Figure 13. The high He/dpa ratio stems from the fact that the reactor vessel and core barrel will be shielded by the graphite reflector assembly and hence will be exposed to a thermalized spectrum, leading to boron and nickel transmutation to He. All tests described below will be performed on the base materials (Alloy 316H) and the weld filler metal (ER16-8-2).

2.5.3.1 Irradiation-Induced Embrittlement

The existing published data on austenitic stainless steels indicate that tensile properties at temperatures from 550°C to 650°C are relatively unaffected by < 0.1 dpa and ~10 appm of He when tested at moderate or high strain rates (>10^{-3} s-1). For example, a compilation of tensile data in Reference 51 indicates virtually no change in yield strength or tensile elongation ≤0.1 dpa for several austenitic stainless steels, including Alloy 316 variants. Similarly, fracture toughness remains high in austenitic stainless steels below 0.1 dpa, with values in excess of 100 MPa√m (Reference 52). While most fracture toughness studies focus on LWR conditions (Figure 14), those data indicate that fracture toughness remains high at ~0.1 dpa. Work by Bernard on Alloy 316H (Reference 53) and DeVries on Alloy 304 (Reference 54) at 550°C confirm that fracture toughness is high at conditions of the KP-FHR operation with JIC values near 100 kJ/m2. In Figure 14, the apparent increase in toughness at 0.3 dpa may be due to some irradiation-induced hardening before any appreciable loss in ductility, which is reasonable based on the tensile data of Nagae (Reference 51). Based on these literature data, no additional tensile or fracture toughness studies are planned.

However, when testing at low strain rates, stainless steel properties can degrade due to helium embrittlement. An example study of the effect of strain rate and temperature on ductility of an austenitic stainless steel is shown in Figure 15 (Reference 55). As shown in Figure 15, tensile ductility remains unaffected at strain rates ≤ 10^{-2} s-1 but slowly degrades as strain rate is lowered, especially in the temperature regime of ~500-700°C. To better assess this effect, literature-reported changes in creep properties after low-dose irradiation in Alloy 316 and Alloy 316 weld metals are summarized in Figure 16. While the data show some scatter, creep strength can decrease by up to ~ 30% after irradiation. Meanwhile, creep ductility is shown to either increase or decrease by up to 20% (in base metal) or 70% (in weld metal) after irradiation.

In order to better define a factor of degradation for creep performance, the effects of irradiation on Alloy 316H and ER16-8-2 will be assessed by post-irradiation testing. The irradiation/post-irradiation testing matrix is shown in Table 11. The target irradiation conditions are designed to be bounding in temperatures (550°C and 650°C), dpa (0.1 and 1 dpa), and He (3 and 15 appm) for the KP-FHR reactor vessel [[at]] . Prior to irradiation, the materials will be machined into sub-size specimens typically used for HFIR irradiations. Post-irradiation creep testing will be performed on the specimens irradiated to 650°C and also tested at 650°C, as summarized in Table 12. Testing at the highest temperature is deemed conservative as creep strength degradation is reported to increase mildly with temperature, as seen in Figure 16 for data point from Aoto, L. et al., (Reference 56) and also reported for 10 dpa-irradiated Alloy 316 (Reference 57). Three stress levels and duplicate specimens will be tested to establish a robust stress/life trend. The results from all post-irradiation creep tests will be compared to unirradiated measurements generated using the exact same specimen geometry and test condition. All specimens will be further characterized via optical and electron microscopy to document any changes in slip and fracture modes.

2.5.3.2 Irradiation-Affected Corrosion

Corrosion in KP-FHR could be affected by irradiation through irradiation-induced changes in the redox potential of Flibe, irradiation-induced changes in the corrosion resistance of stainless steel, or both. In water-based systems, both mechanisms (water radiolysis and defect production in stainless steel) are thought to lead to irradiation-accelerated corrosion (Reference 58). However, these mechanisms are not applicable to the KP-FHR environment. First, Flibe is highly resistant to radiolysis because of the rapid recombination of ions in the molten state. Second, while irradiation could affect the chemistry of Flibe through transmutation, the chemistry control system will have the capability to adjust the redox potential of the salt and correct changes induced by transmutations, expected to be very small. Third, irradiation-induced defect in stainless steel can lead to radiation-enhanced diffusion, which may affect corrosion, but because of the high operating temperature of 550°C and the dpa rate of 0.1 dpa / 20 y (i.e., 10^{-10} dpa/s), the vacancy concentration is not significantly affected by irradiation, and radiation-enhanced diffusion is expected to be minimal.

Existing data indicates that irradiation effects are limited and can be both negative and positive. For example, Lei et al., show a modest increase in post-irradiation bulk corrosion rates (~3X faster) in FLiNaK salt after ~6.18 dpa irradiation with helium ions (Reference 59). In contrast, recent work by Short et al., indicates that simultaneous irradiation and corrosion in FLiNaK acts to minimize intergranular corrosion in molten salt (Reference 60 and 61). Apparently, increased near-surface vacancy concentrations from irradiation accelerates general corrosion (likely controlled via bulk diffusion) but increased intragranular vacancies promotes diffusion from grain interiors to the grain boundary, effectively lowering grain boundary corrosion rates. Note that once recent study by MIT suggests that the combined effects of neutron irradiation and graphite could be as a large as 10X (Reference 62). However, Kairos Power notes that in that research, the gas lines that provided shielding of the salt were plugged during the experiment, likely causing contamination by oxidizing impurities (Reference 63 and 64). For that reason, Kairos Power discounts the suggested factor of 10X.

Given that: (1) the only safety-related component that is subject to irradiation is the thick-walled reactor vessel, (2) the irradiation dose is quite low < 0.1 dpa and (3) irradiation has shown a benefit to grain boundary corrosion (which is the primary concern), no immediate testing is planned. Instead, irradiation

affected corrosion will be assessed via the reliability and integrity management program in the KP-FHR (Appendix B). This plan will utilize surveillance coupons and component monitoring to confirm that the effect of irradiation on corrosion is non-existent or manageable.

2.5.3.3 Irradiation-Assisted Stress Corrosion Cracking (IASCC)

Similar to irradiation affected corrosion, IASCC is not an expected degradation mode in the KP-FHR. The two main pathways for IASCC in water environments are radiation effects on the water chemistry and on the materials (Reference 65). In the KP-FHR environment:

- Radiolysis of Flibe is not a concern, as detailed in in Section 2.5.3.2, and no irradiation-induced changes in the corrosion potential is expected;

- The accumulated dpa in the reactor vessel of <0.1 dpa, which is lower than the lower bound of ~0.3 dpa for IASCC observed in boiling water reactors (Reference 65).

Furthermore, without significant hardening in the alloys at 0.1 dpa (Reference 51), and a potential benefit to grain boundary corrosion rates (Reference 60 and 61), it is unclear how irradiation would increase susceptibility to IASCC. Since there is no direct concern for stress corrosion cracking and only limited means by which irradiation could increase susceptibility (i.e., no expected effect on the coolant chemistry, only slight hardening at 0.1 dpa), no direct IASCC testing is planned at this time. Instead, the KP-FHR reliability and integrity management (RIM) program will assess this area via surveillance coupon and component monitoring.

3 CONCLUSIONS AND LIMITATIONS

3.1 CONCLUSIONS

Kairos Power has selected Alloy 316H base metal and ER16-8-2 weld filler metal as the metallic structural alloys for use in safety-significant, high temperature, component design. This report presents the qualification for those two alloys. The results of the expert panel PIRT review concluded that additional investigation is required to support qualification. Specifically: (1) extending the ASME qualification of ER16-8-2 weld metal to higher temperature and (2) assessing potential environmental degradation of both the base metal and weld filler metal.

The weld filler material, ER16-8-2, requires additional investigation to extend the upper temperature limit of the ASME Section III Division 5 to support use in the KP-FHR. This report describes the testing plans that will be used to develop an ASME Code Case for that purpose.

Regarding environmental effects, additional testing and modelling plans are described in this report to demonstrate compatibility of the metallic structural materials with the environments of the safety-significant components in high temperature environments.

While not required in the KP-FHR design for structural performance considerations, [[ ]] . Appendix A of this report details cladding and coating materials that could be used with safety-related high temperature components of the KP-FHR. Such coatings do not affect structural performance of the underlying base metals and will be used consistent with ASME Section III code requirements.

Appendix B presents the framework for an inspection and aging management plan. Kairos Power intends to develop a reliability and integrity management (RIM) plan in accordance with ASME Section XI Division 2. However, as this methodology is under development, Appendix B outlines the intended strategy. The RIM for the KP-FHR will be addressed as part of the safety analysis reports submitted with future licensing applications. Appendix C discusses how statistical analysis of the test data (such as corrosion rates) will be performed and Appendix D presents additional details on the corrosion and environmentally assisted cracking test systems.

Kairos Power is requesting Nuclear Regulatory Commission review and approval of the qualification plan described in this report, subject to the limitations below, for metallic structural materials used for safety-significant high temperature components of the KP-FHR for use by licensing applicants under 10 CFR 50 or 10 CFR 52. The qualification plan for these materials support conformance, in part, to PDC 14 and PDC 31; and the requirements to describe new and novel features required by 10 CFR Part 50, Sections 50.34(a)(1)(ii)(C), 50.34(a)(2), 10 CFR 50.34(b)(4); and to 10 CFR Part 52, Sections 52.79(a)(2) and equivalent regulations in 52.47, 10 CFR 52.137, and 10 CFR 52.157.

3.2 LIMITATIONS

This report is limited to the qualification of metallic structural materials (316H and ER16-8-2) for safety-significant, high temperature components in Flibe wetted areas of the KP-FHR.

4 REFERENCES

1. United States Nuclear Regulatory Commission, Regulatory Guide 1.203, *Transient and Accident Analysis Methods*, December 2005. (ML053500170).

2. Barua, B., et al. (2020). *Acceptance Criteria for the Mechanical Integrity of Clad/Base Metal Interface for High Temperature Nuclear Reactor Cladded Components*. Pressure Vessels & Piping. Minneapolis, MN USA, ASME: 1-8.

3. University of California Berkeley Nuclear Engineering. *Fluoride Salt Cooled High Temperature Reactor.* 2015.. [ONLINE] Available at:http://fhr.nuc.berkeley.edu. [Accessed 25 June 2020].

4. Kairos Power, LLC, *Design Overview of the Kairos Power Fluoride Salt Cooled, High Temperature Reactor,* KP-TR-001-P, Revision 1. February 2020. (ML20045E423).

5. Kairos Power, LLC, *Risk-Informed Performance Based Licensing Basis Development Methodology*, KP-TR-009-NP, April 2020. (ML20101P623).

6. Kairos Power, LLC, *Reactor Coolant for the Kairos Power Fluoride Salt-Cooled High Temperature Reactor,* KP-TR-004-P, *Revision 1*. January 2020. (ML20016A486).

7. Kairos Power, LLC, *Principal Design Criteria for the Kairos Power Fluoride Salt Cooled High Temperature Reactor*, KP-TR-003-NP-A. June 2020.

8. Koger, J.W., *Evaluation of Hastelloy N Alloys After Nine Years Exposure to Both a Molten Fluoride Salt and Air at Temperatures from 700 to 560°C*. 1972, Oak Ridge National Laboratory. p. 1-44.

9. McCoy, H. E. and B. McNabb, *PostIrradiation Examination of Materials from the MSRE*, 1972, Oak Ridge National Laboratory. p. 1-104.

10. DeVan, J.H. and R.B. Evans, *Corrosion Behavior of Reactor Materials in Fluoride Salt Mixtures*. 1962, Oak Ridge National Laboratory.

11. Delpech, S., et al., *Molten Fluorides for Nuclear Applications.* Materials Today, 2010. 13(12): p. 34-42.

12. Walters, L., et al., *Sodium Fast Reactor Fuels and Materials: Research Needs*. 2011, Sandia National Laboratory. p. 1-74.

13. Mathew, M.D., R. Sandhya, and K. Laha, *Development of Structural and Steam Generator Materials for Sodium Cooled Fast Reactors.* Energy Procedia, 2011. 7: p. 250-256.

14. Courouau, J.-L., et al., *Corrosion by Liquid Sodium of Materials for Sodium Fast Reactors: the CORRONa Testing Device*, in *ICAPP*. 2011: Nice, France. p. 1-11.

15. Keiser, J.R., *Status of Tellurium-Hastelly N Studies in Molten Fluoride Salts*. 1977, Oak Ridge National Laboratory. p. 1-31.

16. Keiser, J.R., J.H. DeVan, and E.J. Lawrence, *Compatibility of Molten Salts with with Type 316 Stainless Steel and Lithium.* Journal of Nuclear Materials, 1979. 85&86: p. 295-298.

17. Koger, J.W., *Alloy Compatibility with LiF-BeF_2 Salts Containing ThF_4 and UF_4*. 1972, Oak Ridge National Laboratory. p. 1-52.

18. Zheng, G., et al., *Corrosion of 316 Stainless Steel in High Temperature Molten Li_2BeF_4 (FLiBe) Salt.* Journal of Nuclear Materials, 2015. 461: p. 143-150.

19. McCoy, H. E. and B. McNabb (1972), *Intergranular Cracking of INOR-8 in the MSRE*, Oak Ridge National Laboratory: 1-185.

20. McCoy, H.E., *Status of Materials Development for Molten Salt Reactors*. 1978, Oak Ridge National Laboratory. p. 1-38.

21. Ignatiev, V. and A. Surenkov, *Alloys Compatibility in Molten Fluorides: Kurchatov Institute Related Experience.* Journal of Nuclear Materials, 2013. 441: p. 592-603.

22. Ignatiev, V., et al., *Intergranular Tellurium Cracking of Nickel-Based Alloys in Molten Li, Be, Th, U/F Salt Mixture.* Journal of Nuclear Materials, 2013. 440: p. 243-249.

23. Cheng, H., et al., *Effects of Te on Intergranular Embrittlement of a Ni-16Mo-7Cr Alloy.* Journal of Nuclear Materials, 2015. 461: p. 122-128.

24. Cheng, H., et al., *EPMA and TEM Characterization of Intergranular Tellurium Corrosion of Ni-16Mo-7Cr-4Fe Superalloy.* Corrosion Science, 2015. 97: p. 1-6.

25. McNeese, L.E., *Molten-Salt Reactor Program Semiannual Progress Report*. 1976, Oak Ridge National Laboratory. p. 1-183.

26. vanRooyen, I.J., et al., *Advanced Electron Microscopy and Micro-Analytical Technique Development and Application on Irradiated TRISO-Coating Particles from the AGR-1 Experiment*. 2017, Idaho National Laboratory.

27. *High-Temperature Characterisitics of Stainless Steels*, N.D. Institute, Editor., American Iron and Steel Institute: A Designer's Handbook Series. p. 1-44.

28. *The Role of Stainless Steel in Petroleum Refining,* Committee of Stainless Steel Producers. January 1, 1977. p. 1-57.

29. *Material Fabrication and Repair Considerations for Austenitic Alloys Subject to Embrittlement and Cracking in High Temperature 565-760°C (1050-1400°F) Refinery Services*. 2012, American Petrochemical Institute. p. 1-63.

30. Williamson, M., *Pyroprocessing Technologies: Recycling Used Nuclear Fuel for a Sustainable Energy Future*. 2019: Argonne National Laboratory.

31. Choi, E.-Y. and S.M. Jeong, *Electrochemical Processing of Spent Nuclear Fuels: An Overview of Reduction in Pyroprocessing Technology.* Progress in Natural Science: Materials International, 2015. 25: p. 572-582.

32. Simpson, M.F., *Developments of Spent Nuclear Fuel Pyroprocessing Technology at Idaho National Laboratory*. 2012, Idaho National Laboratory. p. 1-23.

33. Sim, J.-H., Y.-S. Kim, and I.-J. Cho, *Corrosion Behavior Induced by LiCl-KCl in Type 304 and 316 Stainless Steel and Copper at Low Temperature* Nuclear Engineering and Technology, 2017. 49: p. 769-775.

34. Kondo, M., et al., *Metallurgical Study on Corrosion of Austenitic Steels in Molten LiF-BeF_2 (Flibe).* Journal of Nuclear Materials, 2009. 386-388: p. 685-688.

35. Qiu, J., et al., *Galvanic Corrosion of Type 316L Stainless Steel and Graphite in Molten Fluoride Salt*. Corrosion Science, 2020. 170: p. 1-10.

36. Bradshaw, R.W. and S.H. Goods, *Corrosion Resistance of Stainless Steels During Thermal Cycling in Alkali Nitrate Molten Salts*. 2001, Sandia National Laboratory.

37. ASME, *Boiler and Pressure Vessel Code*, in *High Temperature Reactors*. 2017, American Society of Mechanical Engineers.

38. International, A., *Standard Test Method for Creep-Fatigue Crack Growth Testing*. 2016, ASTM International. p. 1-19.

39. International, A., *Standard Test Methods for Conducting Creep, Creep-Rupture, and Stress-Rupture Tests of Metallic Materials*. 2018. p. 1-14.

40. ASME, *Development of Weld Strength Reduction Factors and Weld Joint Influence Factors for Service in the Creep Regime and Application to ASME Codes*. 2017, ASME. p. 1-376.

41. Kairos Power, LLC, *Quality Assurance Program for the Kairos Power Fluoride Salt-Cooled High Temperature Reactor*, KP-TR-007-NP. May 2020. (ML20136A414).

42. Young, G.A., M.J. Hackett, and T.-L. Sham, *Materials Challenges for Molten Salt Reactors*, in *1st International Conference on Generation IV and Small Reactors*. 2018, CNS: Ottawa, CA. p. 1-17.

43. Henthorne, M., *The Slow Strain Rate Stress Corrosion Cracking Test - A 50 Year Retrospective.* Corrosion. 72(12): p. 1488-1518.

44. International, A., *Standard Practice for Slow Strain Rate Testing to Evaluate the Susceptibility of Metallic Materials to Environmentally Assisted Cracking*, in *G129-00*. 2000, ASTM.

45. Jones, R.H. and R.E. Ricker, *Mechanisms of Stress-Corrosion Cracking*, in *Stress-Corrosion Cracking*, R.H. Johnes, Editor. 1992, ASM International: Metals Park, OH. p. 1-40.

46. Spindler, M.W. and M.C. Smith, *The Effect of Multiaxial States of Stress on Creep Failure of Type 316H Under Displacement Control*, in *Pressure Vessels and Piping Division Conference*. 2009, ASME: Prague, Czech Republic. p. 1-7.

47. Spindler, M., *Materials Issues in Advanced Gas Cooled Reactors*, R. McReynolds, Editor. 2019: British Energy. p. 1-55.

48. Miller, P.D. and W.K. Boyd, *Corrosion of Beryllium*. 1967, Battelle Memorial Institute: Columbus, OH. p. 1-38.

49. Higgins, J., *Precipitation in the Iron-Beryllium System.* Acta Metallurgica, 1974. 22(2): p. 201-217.

50. Zweibaum, N., et al., *Phenominology, Methods, and Experimental Program for Fluoride-Salt-Cooled, High-Temperature Reactors (FHRs).* Progress in Nuclear Energy, 2014. 77: p. 390-405.

51. Nagae, Y., et al., *Irradiation Effect on Mechanical Properties in Structural Materials of Fast Breeder Reactor Plant.* Journal of Nuclear Materials, 2011. 414: p. 205-210.

52. Zinkle, S.J. and G.S. Was, *Materials Challenges in Nuclear Energy.* Acta Materialia, 2013. 61: p. 735-758.

53. Bernard, J. and G. Verzeletti, *Elastic-Plastic Fracture Toughness Characteristics of Irradiated 316H Stainless Steel*, in *Elastic-Plastic Fracture Test Methods: The User's Experience, ASTM STP 856*, E.T. Wessel and F.J. Loss, Editors. 1985, ASTM. p. 131-149.

54. DeVries, M.I. *J-Integral Toughness of Low Fluence Neutron-Irradiated Stainless Steel*. in *13th International Symposium on the Influence of Radiation on Material Properties*. 1987. ASTM.

55. DeVries, M., et al. *Effects of Neutron Irradiation and Fatigue on Ductility of Stainless Steel*. in *Effect of Radiation on Structural Materials*. 1979.

56. Aoto, K., et al., *Effects of Neutron Irradiation on Creep Properties of FBR Grade 316 Stainless Steel*. 1995, International Atomic Energy Agency.

57. Bloom, E.E. and J.O. Stiegler, *On the Microstructure and Creep-Rupture Properties of Type 316 Stainless Steel*, in *STP 529: Effects of Radiation on Substructure and Mechanical Properties of Metals and Alloys*, J. Motef, Editor. 1973, ASTM. p. 360-382.

58. Raiman, S.S., D.M. Bartels, and G.S. Was, *Radiolysis Driven Changes to Oxide Stability During Irradiation-Corrosion of 316L Stainless Steel in High Temperature Water.* Journal of Nuclear Materials, 2017. 493: p. 40-52.

59. Lei, G., et al., *Irradiation Accelerated Fluoride Molten Salt Corrosion of Nickel-Based UNS N10003 Alloy Revealed by X-Ray Absorption Fine Structure.* Corrosion Science, 2020. 165: p. 1-5.

60. Zhou, W., et al., *A Simultaneous Corrosion/Irradiation Facility for Testing Molten Salt-Facing Materials.* Journal of Physics Research B, 2019. 440: p. 54-69.

61. Zhou, W.Y., et al., *Proton Irradiation-Decelerated Intergranula Corrosion of Ni-Cr Alloys in Molten Salt.* Proquest Open Access, 2019: p. 1-11.

62. Forsberg, C.W., et al., *Integrated FHR Technology Development: Tritium Management, Materials Testing, Salt Chemistry Control, Thermal Hydraulics and Neutronics, Associated Benchmarking and Commercial Basis*. 2018, MIT / Berkeley / Wisconsin / New Mexico. p. 1-534.

63. Carpenter, D., et al., *Findings of the Second Round of Fluoride Salt High Temperature Reactor Materials Irradiation Tests at the MIT Research Reactor, in ICAPP*. 2015: Nice, France. p. 1-10.

64. Carpenter, D.M., et al., *Status of the Fluoride Salt High Temperature Reactor Materials Irradiation Tests at the MIT Research Reactor, in European Research Reactor Conference*. 2015. ENS: Bucharest, Romania. p. 218-227.

65. Was, G.S., *Fundamentals of Radiation Materials Science*. 2007, Berlin: Springer-Verlag.

66. Aktaa J., et al., *Effects of hold time and neutron irradiation on the low-cycle fatigue behaviour of type 316-CL and their consideration in a damage model*. 2002. Nucl Eng Des. 213(2–3):111–117. doi:10.1016/S0029-5493(01)00511-8.

67. Pfeil P., et al., *Effects of irradiation in austenitic steels and other high-temperature alloys. In: Flow and Fracture of Metals and Alloys in Nuclear Environments*. 1965. ASTM International.

68. Tavassoli A-A., et al., *Data Collection on the Effect of Irradiation on the Mechanical Properties of Austenitic Stainless Steels and Weld Metals*. 1996. Eff Radiat Mater 17th Int Symp.:995-995–15. doi:10.1520/stp16521s.

69. Ward AL., *Thermal and irradiation effects on the tensile and creep rupture properties of weld deposited type 316 stainless steel*. 1974. Nucl Technol. 24(2):201–215. doi:10.13182/NT74-A31475.

70. Messner, M.C., et al., *Finite Element Analysis of Compliant Cladding and Base Metal Systems*. 2018, Argonne National Laboratory.

71. Messner, M.C., et al., *The Mechanical Interaction of Clad and Base Metal for Molten Salt Reactor Structural Components*, in *ASME Pressure Vessels and Piping*. 2018.

72. Barua, B., et al., *Development of Design Method for High Temperature Nuclear Reactor Cladded Components*, in *Pressure Vessels & Piping*. 2020, ASME: Minneapolis, MN, USA. p. 1-8.

73. Barua, B., et al., *Selection Criteria for Clad Materials to Use with a 316H Base Material for High Temperature Nuclear Reactor Cladded Components*, in *Pressure Vessels & Piping*. 2020, ASME: Minneapolis, MN, USA. p. 1-9.

Table 1. Summary of Key Parameters for the KP-FHR

Parameter	Value/Description
Reactor Type	Fluoride-salt cooled, high temperature reactor (FHR), pool-type
Core Configuration	Pebble bed core, graphite moderator/reflector, and enriched Flibe molten salt coolant
Physical Dimensions	Reactor Vessel is [[ ]]
Reactor Thermal Power	320 MW_{th}
Primary Heat Transport System	Flibe Salt, 550°C-650˚C, ~0.2 MPa, [[ ]]
Intermediate Heat Transport System	Nitrate Salt, [[ ]]
Power Conversion System	[[ ]]
Material for Safety-Related Structures	ASME Section III, Division 5, approved

Table 2. Ranking of Structural Alloys of Interest to the KP-FHR

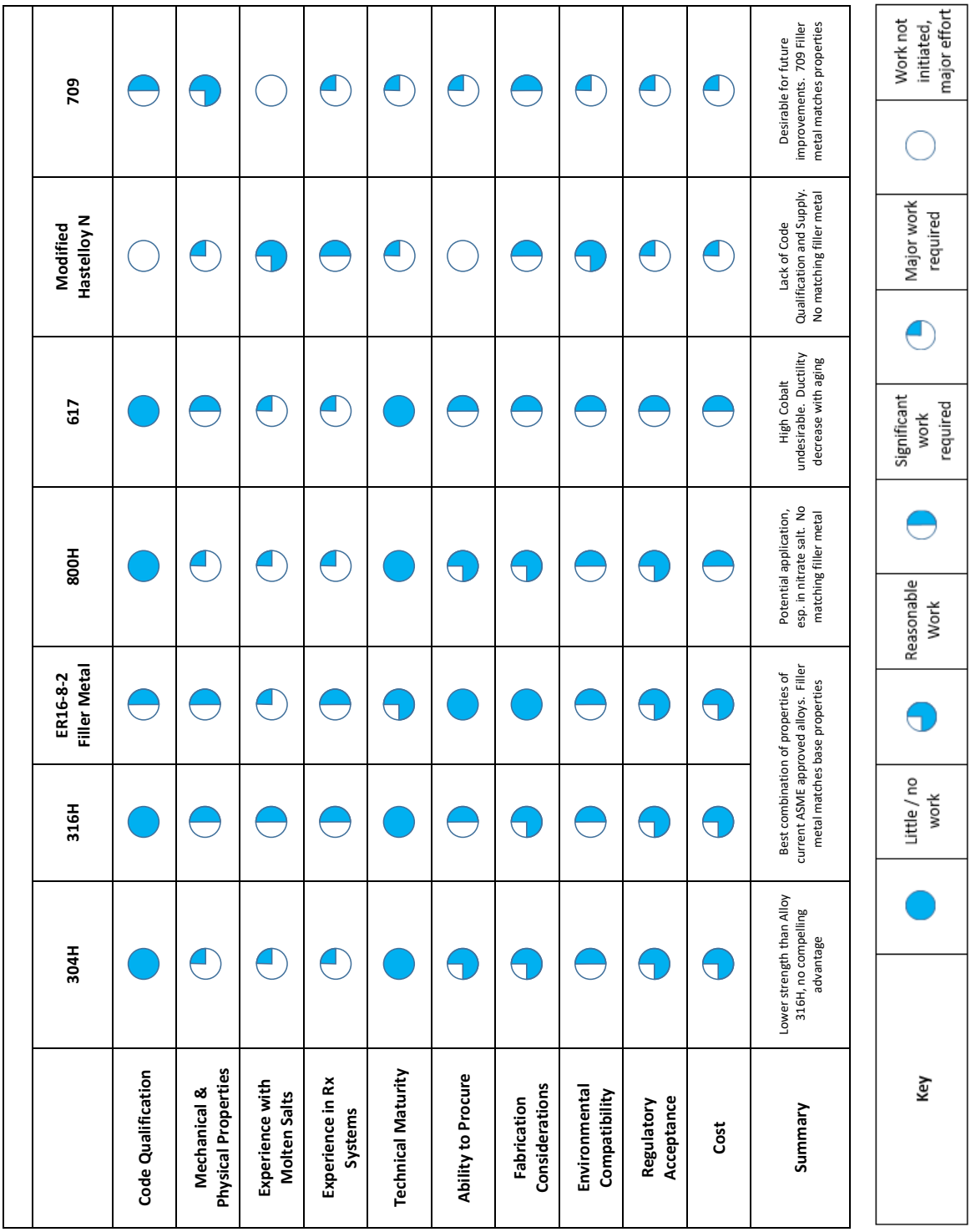

Table 3. Summary of Tests to Extend the ASME Qualification of ER16-8-2

[[

]]

Table 4. Summary of Testing to Address Environmental Degradation Phenomena

Category	Phenomena	Test Description	Major Variables
Corrosion	General Corrosion	Coupon exposure	Testing at 600-700°C up to 10,000 hours. Impurity additions. Redox control. *f* (t, T, microstructure, salt composition, flow rate)
	Localized Corrosion	Creviced coupon exposure	650°C in nominal Flibe
	Erosion / Wear	Coupon exposure	650°C in nominal Flibe
	Cold Leg Occlusion	Coupon exposure and system characterization	600-700°C in nominal Flibe
Environmentally Assisted Cracking	Stress Corrosion Cracking	Both slow strain rate tensile samples and pre-cracked fracture-mechanics based tests	SSRT: 600-700°C in nominal Flibe, stroke rates 10^{-6}-$5x10^{-8}$
			SCC: 600-700°C in nominal Flibe, range of mechanical conditions
	Environmental Creep	In-situ uniaxial samples	600-700°C, at least two stress levels to compare to air data
	Corrosion Fatigue	Fracture-mechanics based tests	Data from environmental pre-crack of the SCC sample
'Other'	Stress relaxation cracking	Ex-situ (air) testing of tensile samples with varying triaxiality	Testing as a function of temperature and triaxial stress. Directly assess effect of post weld heat treat
	Phase Formation Embrittlement	Coupon exposure and characterization	Prototypical Be and graphite in Flibe
	Thermal Cycling / Striping	Primarily assessed via analysis	Primarily computational analysis. Testing only if required
Irradiation Effects	Irradiation Affected Corrosion	Assess via surveillance sample program	Alloy 316H and ER16-8-2 assessed in surveillance program
	Irradiation Affected Stress Corrosion Cracking		
	Irradiation-Induced Embrittlement	Ex-situ testing for creep degradation factor	Doses of 0.1 and 1 dpa

Table 5. Summary of Testing to Address Corrosion

Purpose		Materials	Environment	Conditions
Effect of temperature on corrosion		Alloy 316H and ER 16-8-2	Nominal Flibe	600,650,700°C 1,000-10,000 hours
Effect of microstructure	Welding	Alloy 316H heat affected zone	Nominal Flibe	650°C 1,000-10,000 hours
	Plastic Strain	20% cold worked Alloy 316H and ER 16-8-2	Nominal Flibe	600°C 1,000-10,000 hours
	Aging	Alloy 316H and 16-8-2, aged 10,000 hrs	Nominal Flibe	650°C 1,000-10,000 hours
	Post Weld Heat Treatment	Alloy 316H, Heat Affected Zone, ER 16-8-2	Nominal Flibe	650°C 1,000-10,000 hours
Effect of contaminants		Alloy 316H and ER 16-8-2	Nominal Flibe + nitrate and water	650°C 1-week contamination
Effect of redox control		Alloy 316H and ER 16-8-2	Nominal Flibe + [[ ]]	700°C 1,000-10,000 hours
Effect of occluded geometry		Alloy 316H and ER 16-8-2	Nominal Flibe	650°C 1,000-10,000 hours
Effect of erosive flow		Alloy 316H and ER 16-8-2	Nominal Flibe + graphite particulate	650°C 1,000-10,000 hours

Table 6. Summary of Slow Strain Rate Testing

Materials	Environment	Temperature (°C)	Stroke Rates (in/in)/sec
Alloy 316H Annealed & WQ ER16-8-2 As Welded	Nominal Flibe	550	10^{-6} - $5x10^{-8}$
		600	10^{-6} - $5x10^{-8}$
		650	10^{-6} - $5x10^{-8}$

Table 7. Summary of Testing to Address Corrosion Fatigue and Stress Corrosion Cracking

Materials	Environment	Target Corrosion Fatigue Conditions[1] (MPa√m)	Approximate Stress Intensity Factor for SCC Testing[2] (MPa√m)	Temperatures
Alloy 316H Annealed & WQ ER16-8-2 As welded	Nominal Flibe	K_{max} 25 → 15 R=0.9 1 Hz Sine wave	25	550
				650

[1] Corrosion fatigue tests will extend the crack approximately 100 mils under the target conditions
[2] The constant K portion of the test will be held and monitored for at least 90 days to assess if cracking occurs

Table 8. Summary Testing to Address In-situ Creep-Rupture

Materials	Environment	Temperature	Applied Stress
Alloy 316H Annealed & WQ	Flibe + Graphite + Redox Control	550	2 stresses corresponding to failure times of approximately 500 and 2000 hours. Replicate tests conducted at selected conditions
		650	
ER16-8-2 As Welded	Flibe + Graphite + Redox Control	550	
		650	

Table 9. Summary Testing to Assess Stress Relaxation-type Weld Cracking in Alloy 316H

Materials	Conditions	Temperature	Notch Radii (mm)				
Alloy 316H	Weld Thermal Cycle (WTC)	500	5.66	2.00	1.24	0.60	0.20
		550	5.66	2.00	1.24	0.60	0.20
		600	5.66	2.00	1.24	0.60	0.20
	WTC + Post Weld Heat Treat	500	5.66	2.00	1.24	0.60	0.20
		550	5.66	2.00	1.24	0.60	0.20
		600	5.66	2.00	1.24	0.60	0.20
Alloy 347	Weld Thermal Cycle (WTC)	500	5.66	2.00	1.24	0.60	0.20
		550	5.66	2.00	1.24	0.60	0.20
		600	5.66	2.00	1.24	0.60	0.20

Table 10. Summary Testing to Assess Carbon and [[ ]] Pickup in Alloy 316H

Test Type	Materials	Environment	Temperature (°C)	Comment
Corrosion Coupon	Alloy316H	Flibe + Graphite + [[ ]]	650	Conservative test (high T, [[ ]], at least 1000 hours exposure
SSRT	Alloy 316H + ER16-8-2	Flibe + Graphite + [[ ]]	650	$5x10^{-8}$ in/in test to compare with nominal Flibe
In-Situ Creep	Alloy 316H + ER16-8-2	Flibe + Graphite + Redox Control	550 650	Planned tests in redox control will be examined for [[ ]]

Table 11. Irradiation Test Matrix Conditions

Irradiation Temperature (°C)	Target Dose (dpa)	Target He Concentration (appm)	Post-Irradiation Testing
650	0.1	3	Creep
	1	15	

Table 12. Post-Irradiation Thermal Creep Test Conditions

Irradiation Conditions			Out of Pile Test Conditions			
T (°C)	**Doses (dpa)**	**He (appm)**	**T_{test} (°C)**	**Test**	**Creep Stress (MPa) (approx.)**	**Expected unirradiated life (hr) (Reference 61)**
650	0.1	3	650	Thermal Creep	72	30,000
					88	10,000
	1	15			108	3,000
At least two samples per set of conditions will be tested						

Figure 1. Illustration of the Temperature and Irradiation Damage Regime of the KP-FHR Relative to Several Other Reactor Types

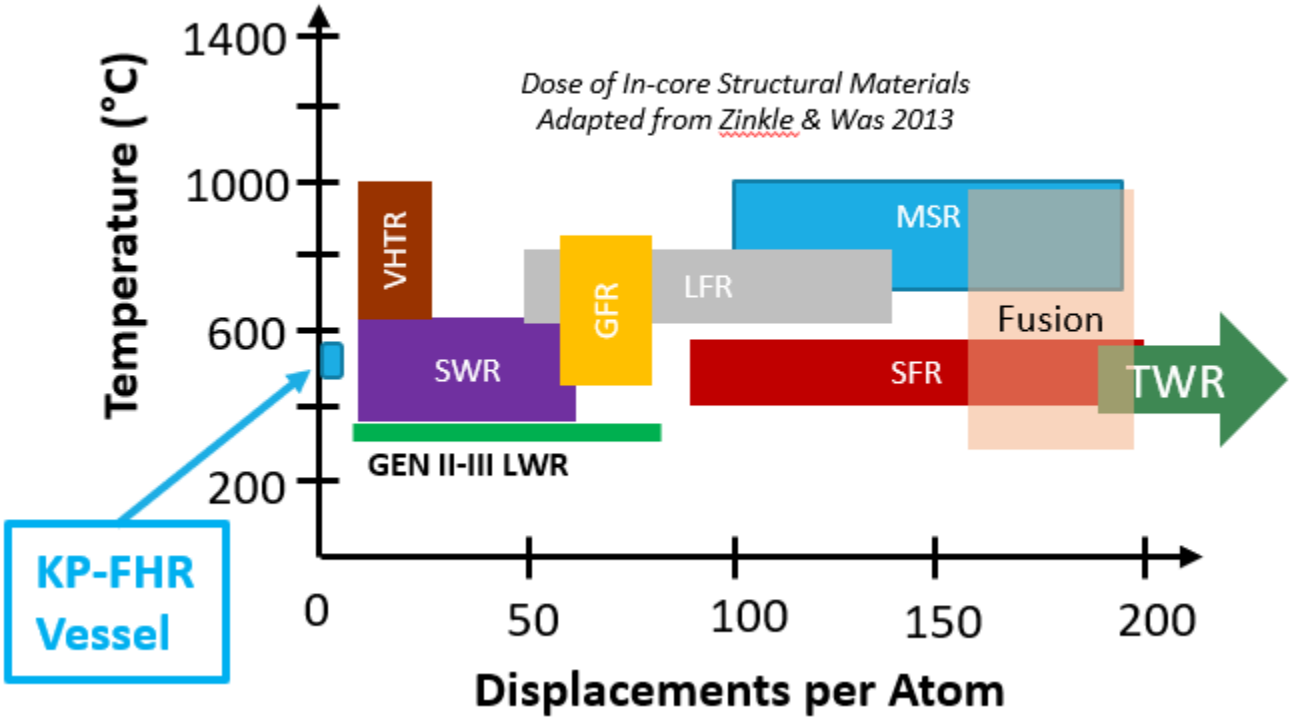

Adapted from Reference 52

Figure 2. Overview of the KP-FHR Heat Transport Loops with Nominal Operating Temperatures.

[[

]]

Figure 3. Comparison of the Operating Pressures and Temperatures of Selected Conventional and Advanced Reactor Designs

[[

]]

Note: The labels refer to pressurized water reactors (PWR), boiling water reactors (BWR), high temperature gas reactors (HTGR), and sodium fast reactors (SFR)

Figure 4. Comparison of the Operating Conditions of Alloy 316H in the KP-FHR (blue box) with Oil & Gas Refinery Components and Existing Creep Rupture Data

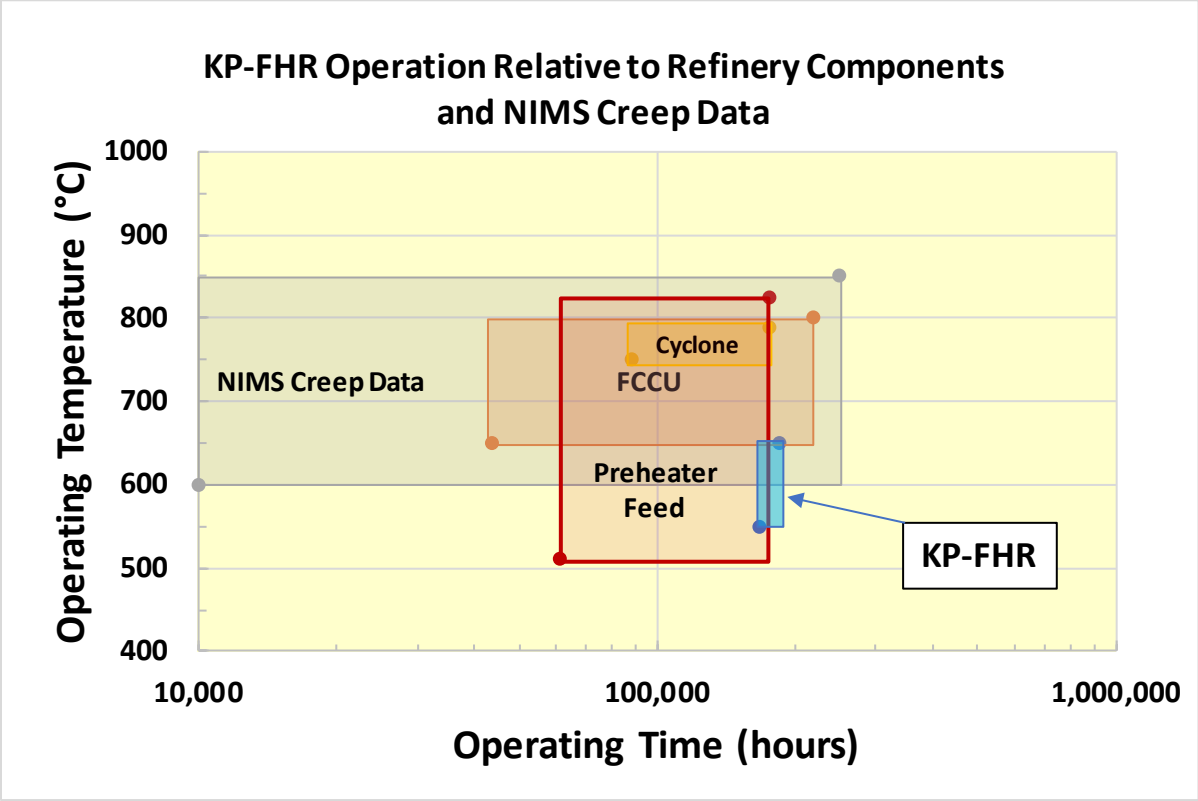

Note: Application of Alloy 316H and its weld metals in the KP-FHR is consistent with industrial practice

Figure 5. Summary of Literature Data for Alloy 316 Corrosion in Molten Flibe

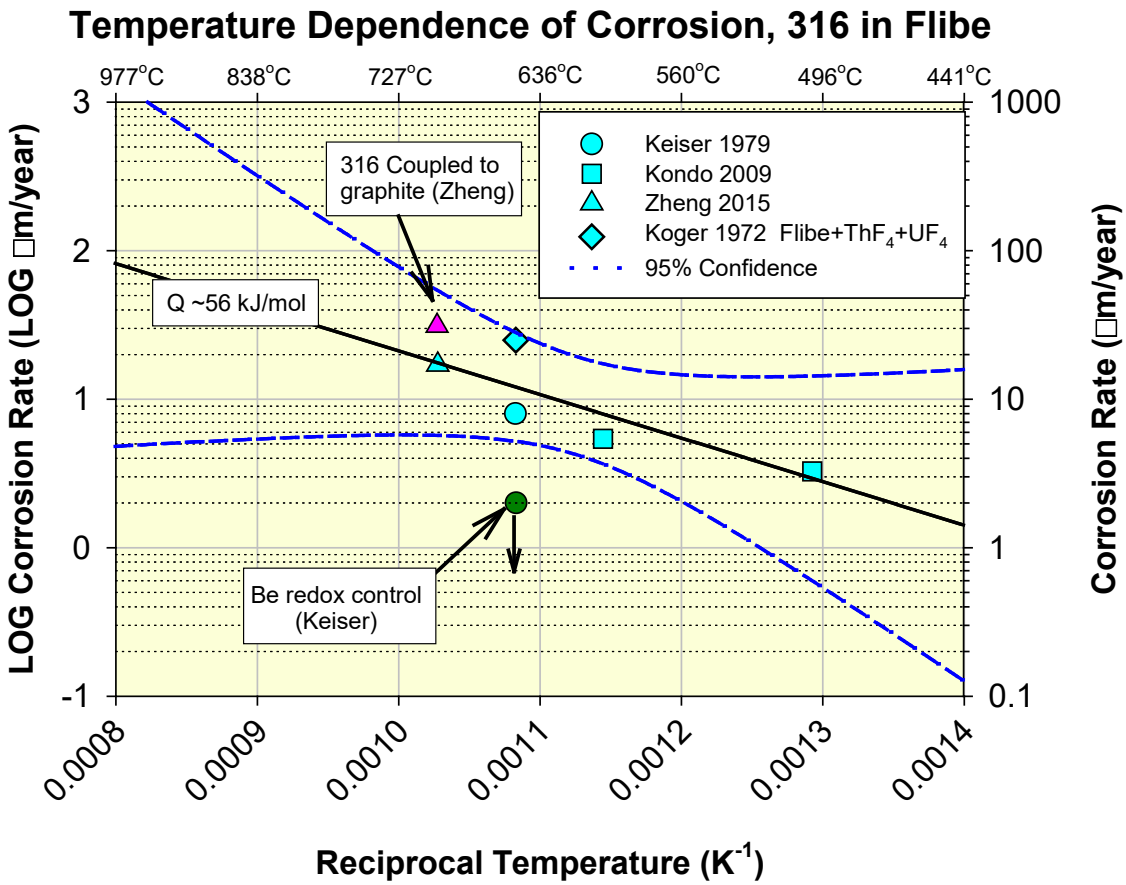

Figure 6. Illustration of the Environmental Degradation Mechanisms Considered in the Kairos Power PIRT Review of Environmental Degradation

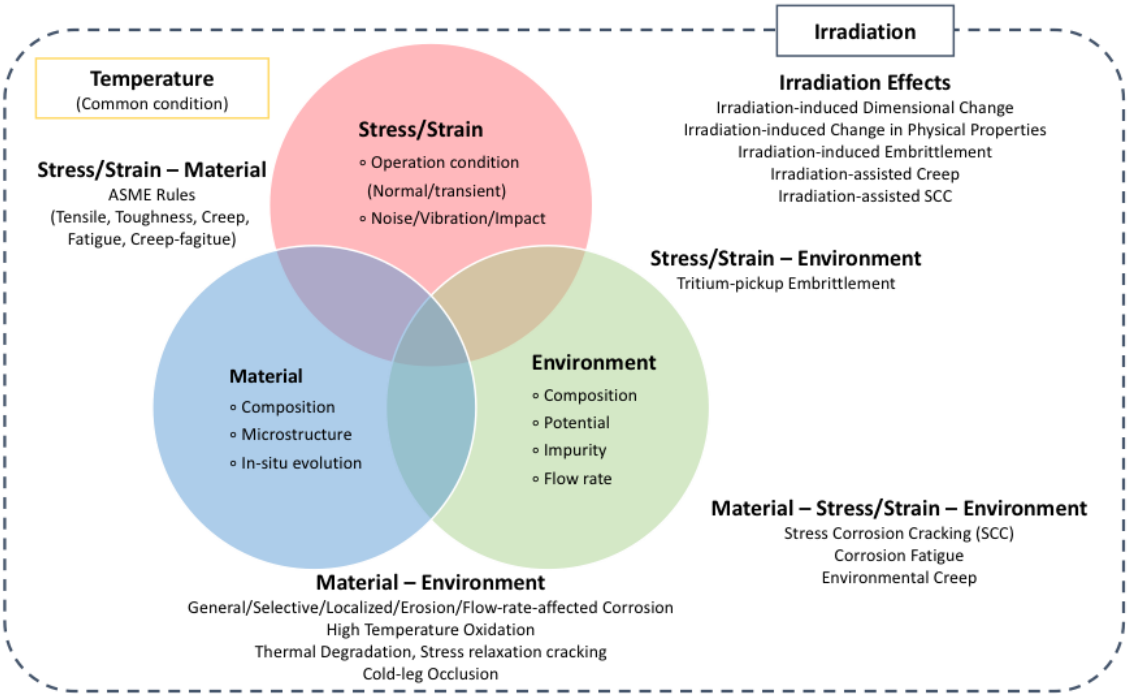

Figure 7. The Knowledge and Importance Rankings Used by the Expert Panel to Assess Environmental Degradation Phenomena

		Knowledge		
		High	*Medium*	*Low*
Importance	*High*	Category #4	Category #2	Category #1 (most important)
	Medium	Category #6	Category #5	Category #3
	Low	Category #9 (least important)	Category #8	Category #7

Figure 8. Summary of the PIRT rankings

[[

]]

Figure 9. In-situ Testing System (left) and an Enlarged View of the Testing Chamber (upper pink portion) and the Cold Leg (blue piping)

[[

]]

Figure 10. Illustration of Slow Strain Rate Testing (SSRT) Data (left) and How the Results May Be Used to Map Out Regimes of Susceptibility (right).

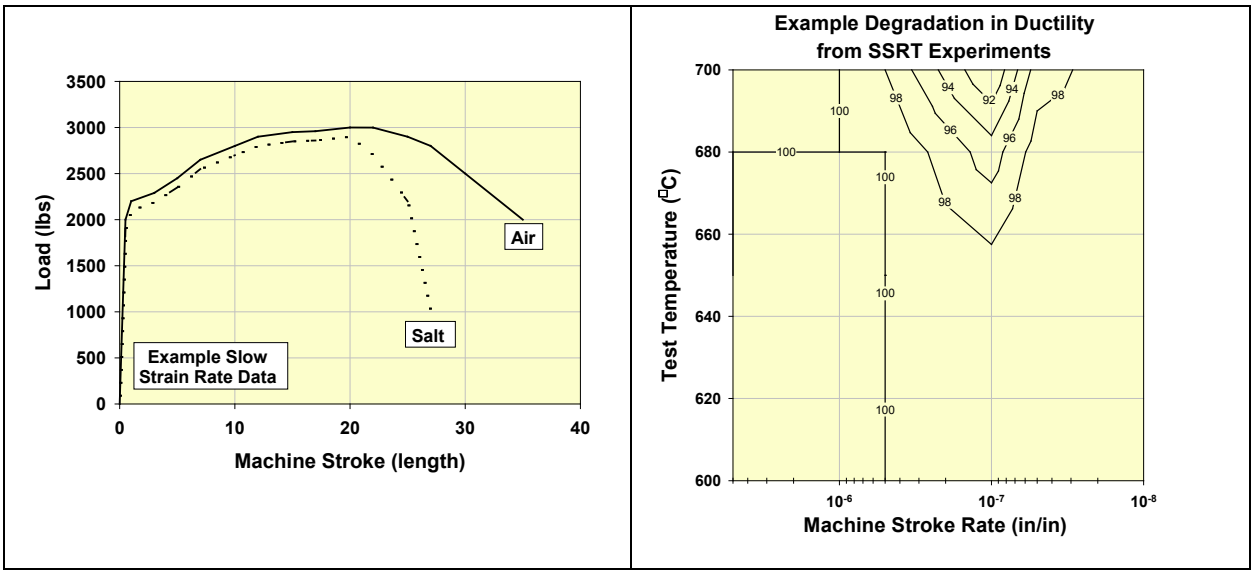

Figure 11. Example Corrosion Fatigue Crack Growth Rate Data (left) and How They Will be Compared to Data Collected in Air (right) to Assess the Effect of Environment

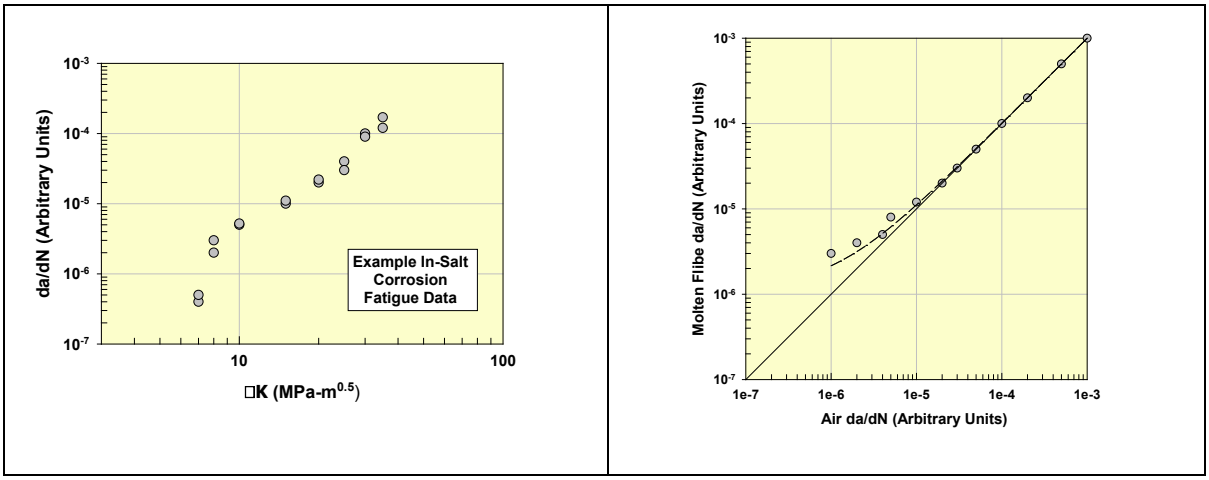

Figure 12. Illustration of a Potential SCC Mechanism in Flibe (top) where Grain Boundary Cr Loss is Accelerated at a Strained Crack Tip and (bottom) Schematic SCC Growth Rate Data

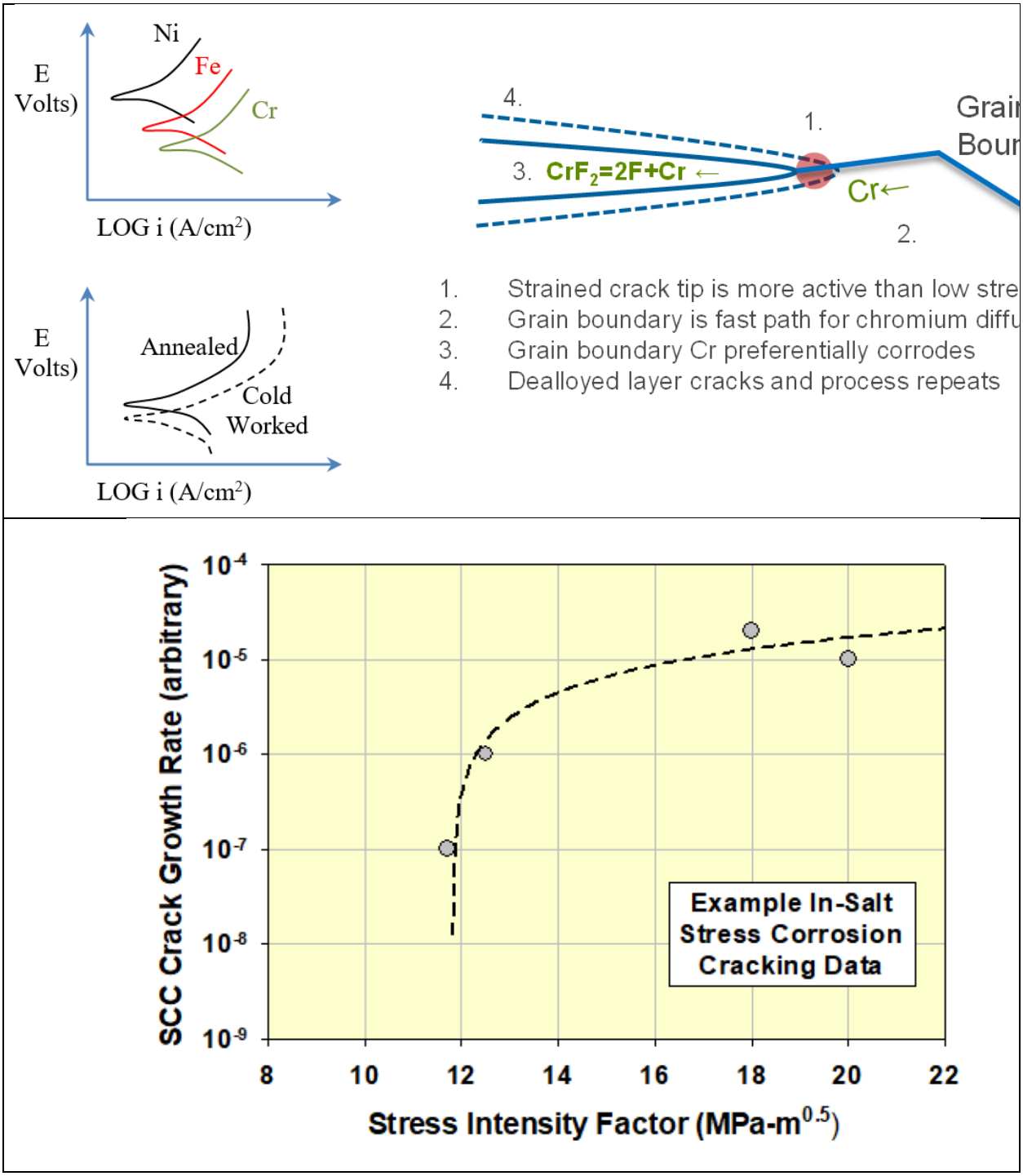

Figure 13. Comparison of the Evolution of Irradiation Damage and Helium Generation in the KP-FHR Reactor Vessel

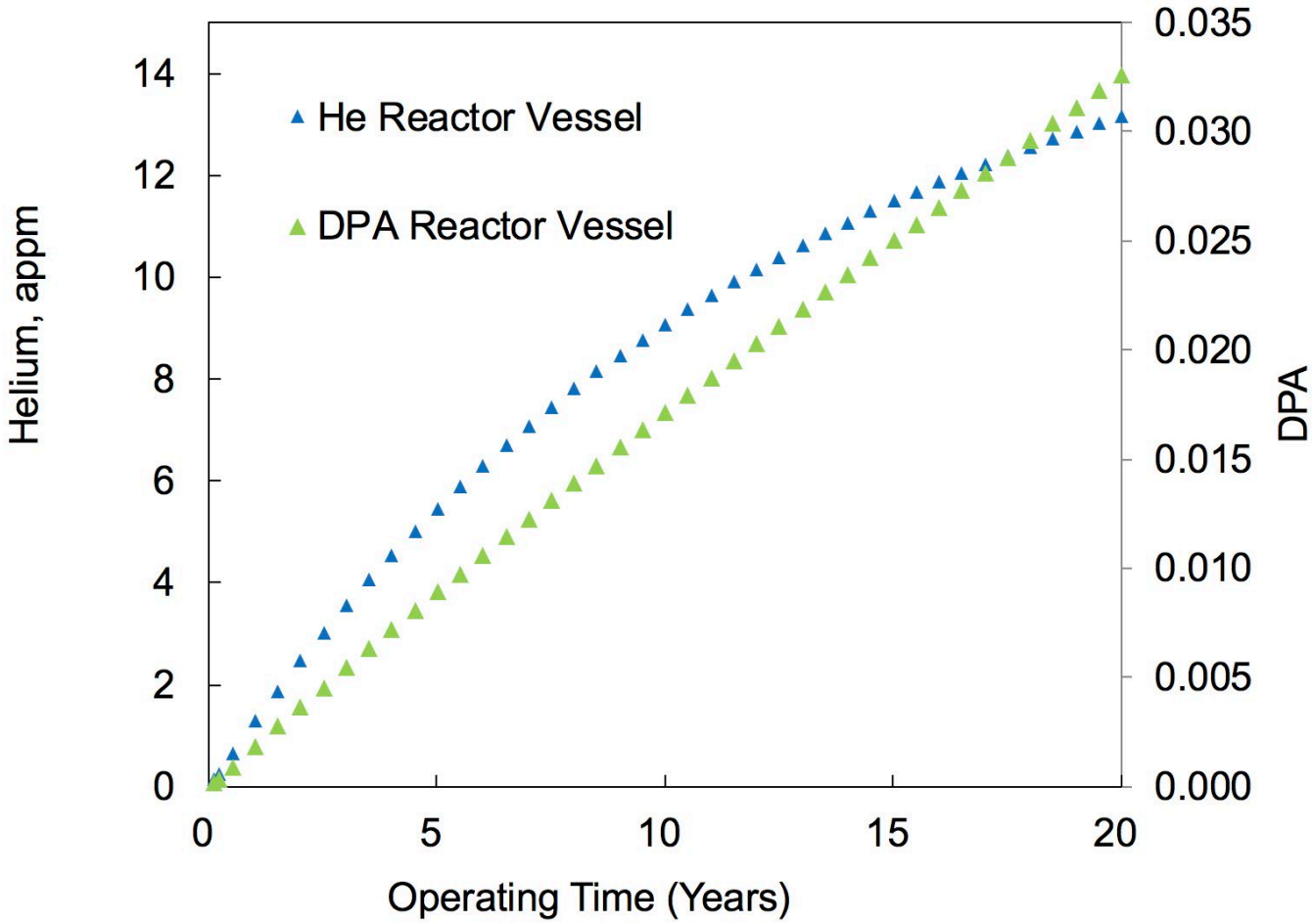

Figure 14. How Irradiation Affects Fracture Toughness in Austenitic Stainless Steels and Specific Data for Alloy 316 and 304 at 550°C.

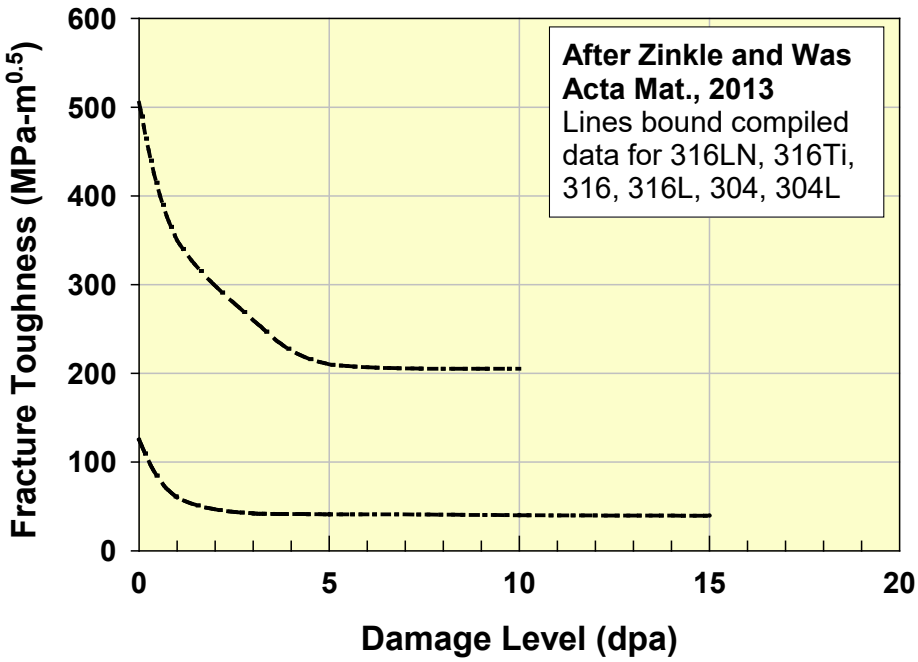

Note: Reference 52

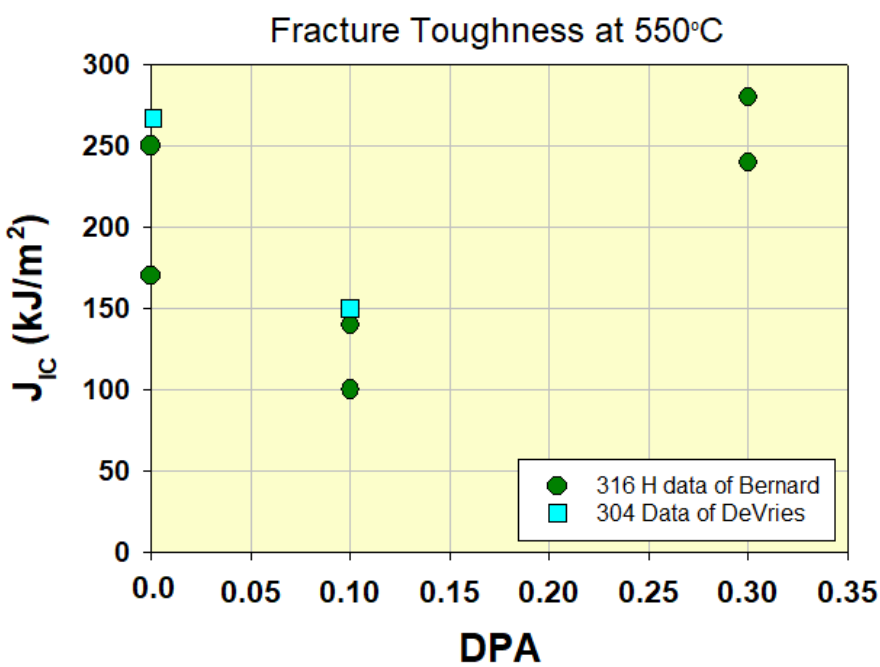

Note: Reference 53 and 54

Figure 15. Illustration of How Strain Rate and Temperature Affect Tensile Ductility in an Austenitic Stainless Steel Irradiated to a Helium Content of ~7 at. ppm

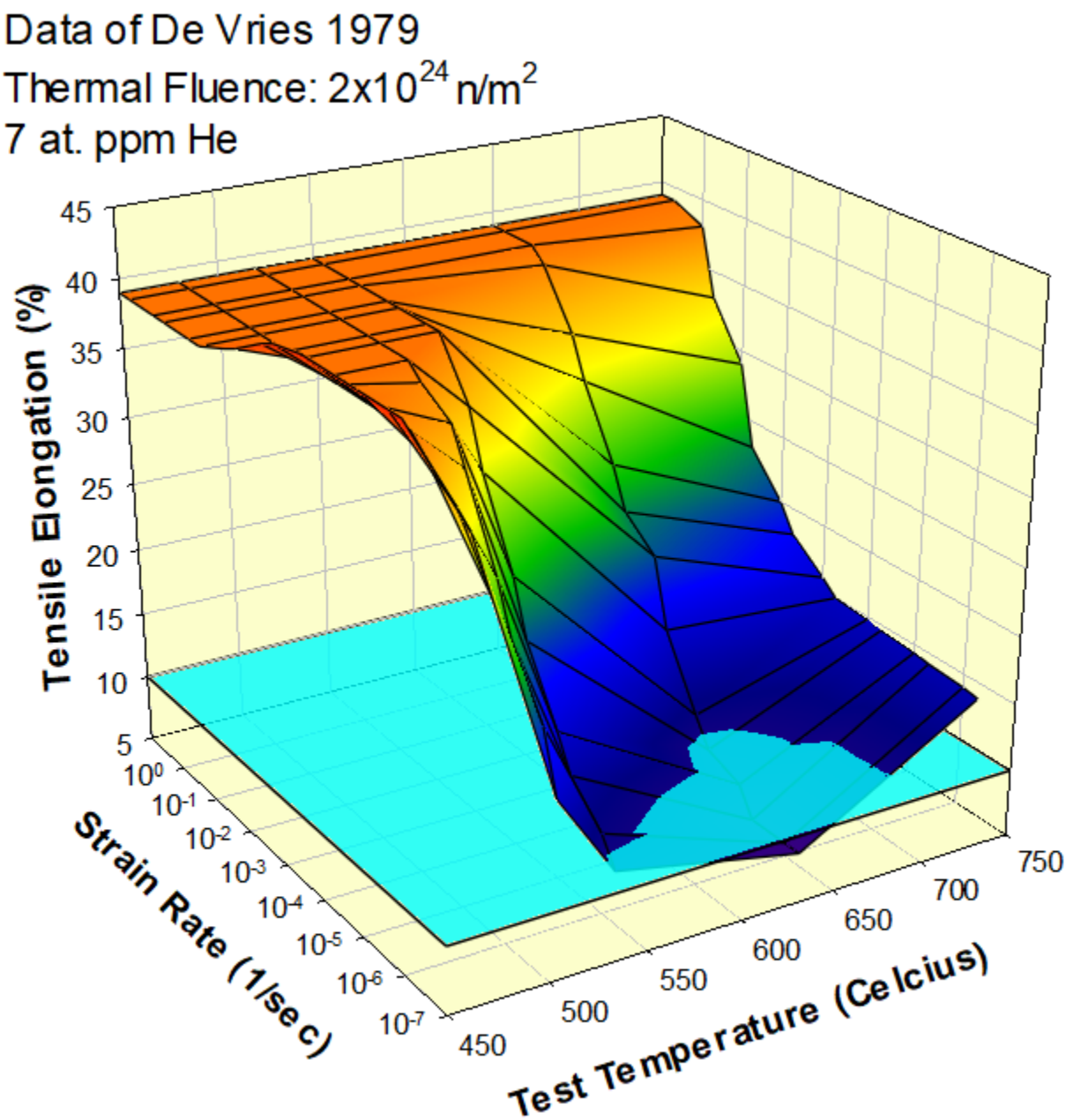

Note: Reference 55

Figure 16. (a) Normalized Creep Strength After Irradiation (Ratio of Irradiated Stress to Unirradiated stress to Reach the Same Average Creep Life) (b) Normalized Creep Ductility After Irradiation (Ratio of Irradiated Ductility to Unirradiated Ductility at the Same Stress

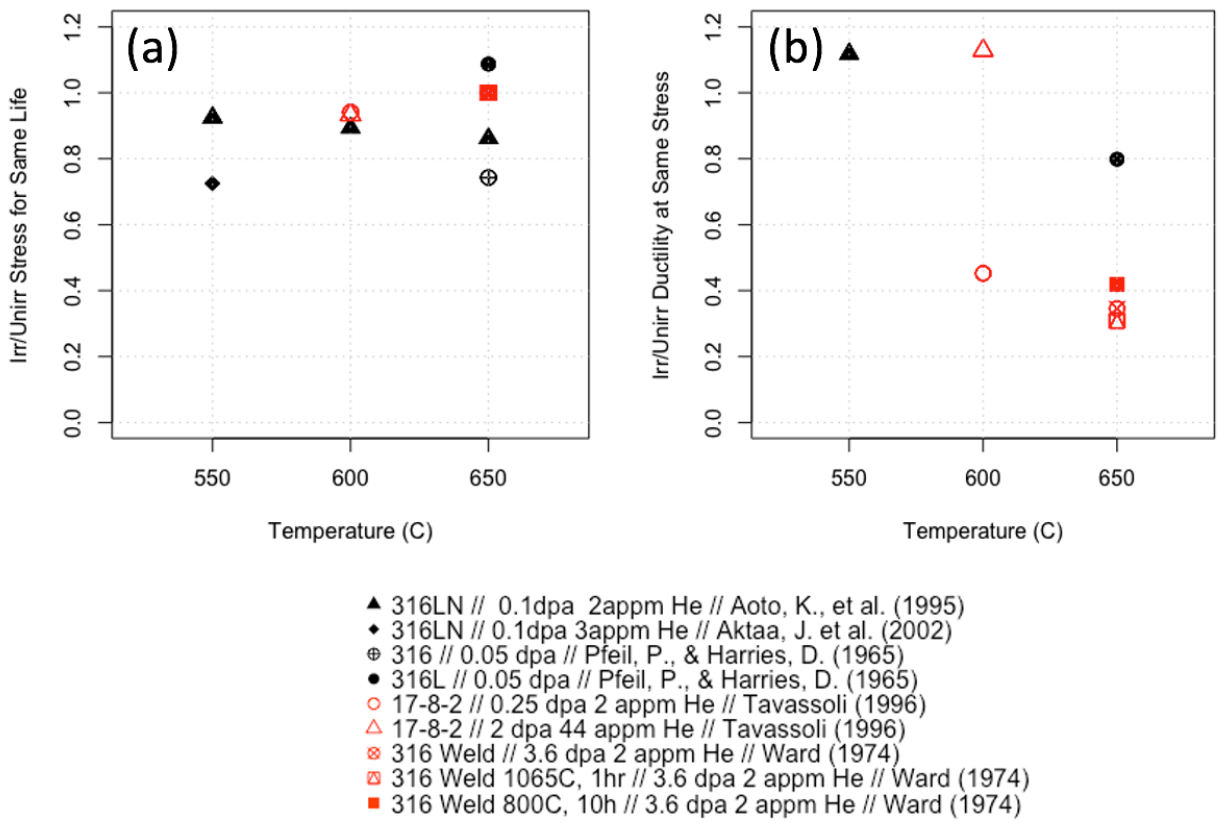

Note: References 56, 66, 67, 68, 69

APPENDIX A. COATINGS AND CLADDING

The design of the KP-FHR does not require the use of cladding or coatings. However, these materials may be desirable to optimize the performance of the reactor system. [[

]] Some cladding & coatings materials of interest are listed in Appendix A, Table 1, for information.

Cladding & Coatings for Salt Facing Applications

Current ASME Section III Division 5 Code rules for cladded structural components in elevated temperature service are limited. ASME Section III Division 5, Paragraph HBB-2121 allows non-Code qualified materials to be used for cladding if the clad thickness is 10% or less of the thickness of the base material. ASME Section III Division 5, Paragraph HBB-3227.8 specifies that no structural strength will be attributed to the cladding in satisfying the primary load stress limits. It also requires that the cladding will be considered in design evaluation related to limits on deformation-controlled quantities, i.e., strain accumulations due to ratcheting and creep-fatigue damage but does not provide guidance or requirements for that assessment. While the 10% clad thickness rule would allow Kairos Power to select corrosion-resistant materials that are not Code qualified for Class A service, the lack of design rules presents challenges in their application.

In order to help enable the application of corrosion-resistant coatings and cladding, Kairos Power is working with Argonne National Laboratory as part of a GAIN research collaboration (References 70, 71, 72, and 73) (Gain cladding project under contract No. DE-AC02-06CH11357 with the US Department of Energy). The GAIN research includes establishing the mechanical nature of the cladding or coating (compliant or elastic), determining key mechanical properties (yield strength, creep rate), assessing the integrity of the coating after thermal cycling, and testing the environmental compatibility of the cladding or coating in molten Flibe salt. While this program is under development, it is expected to result in the ability to use cladding & coatings with ASME Section III Division 5 structural materials.

Cladding & Coatings for Air Side Applications

For the application of cladding or coatings on the air side of safety-related systems, there are no ASME design rules governing their use. Potential applications for coatings on the air side of these systems include oxide films [[ ]] and surface treatments to enhance thermal emissivity. If coatings are used on the air side of safety-related systems, the benefit of the treatment will be demonstrated and confirmed through analysis and/or testing that there is no significant degradation to the underlying structural material.

Appendix A Table 1. Comparison of Selected Coatings & Cladding of Interest to the KP-FHR

[[

]]

APPENDIX B. INSPECTION AND AGING MANAGEMENT

Introduction

Nuclear Power Plant component life management requires a combination of analysis, inspection, testing, and monitoring activities. The information derived from each of these activities complements one another and should be utilized as part of an integrated program. Qualification through mechanical and environmental testing is the first step in ensuring material performance for long-term service in nuclear power plants. While test plans can to some extent account for combinations of mechanical and environmental factors that affect material performance, it is rare that laboratory testing can account for all of the variables and interactions present during reactor operation. Furthermore, it is often impractical to perform laboratory tests for times on the order of the expected component lifetimes (usually decades). While the material qualification test programs described in this document provide confidence that Alloy 316H / ER16-8-2 will perform satisfactorily over the service life of the plant; in-service monitoring and evaluation throughout the plant life will be used to further ensure the safe and reliable operation of the KP-FHR.

Reliability and Integrity Management (RIM)

ASME Section XI has historically provided rules for in-service inspection and the replacement and repair of components during the operating life of light water reactors. The unique physical features of high temperature reactors such as the KP-FHR present a new paradigm for RIM that has required the Code to develop new approaches. The new approach being implemented as ASME Section XI Division 2 “Reliability”, applies to any type of reactor design and was published for the first time in the 2019 Edition of the ASME code.

The new RIM allows a combination of Monitoring and Non-Destructive Examination (MANDE) methods for an aging management program. The ability to use both monitoring and non-destructive examination is a significant advantage to many advanced reactor designs, including the KP-FHR, since their compact size and need for coolant chemistry control limits access to some components during the operating lifetime of the plant. While the 2019 Edition of ASME Section XI Division 2 outlines the top-level requirements for a RIM program, Mandatory Appendix VII of Division 2 will describe the specific MANDE methods and acceptance criteria for each of the different types of advanced reactors. Note that Article VII-4 has been reserved for Molten Salt Reactors (and presumably FHR designs) but has not yet been developed in detail. Kairos Power is active with the Section XI Committee Sub-Groups and Working-Groups related to RIM and MANDE and plans to apply the KP-FHR experience to the development of relevant Code articles for FHRs.

Development of the RIM program for the Kairos Power plant will be performed in accordance with the requirements of ASME Section XI 2019 Edition, Mandatory Appendix I (“RIM Decision flowcharts for use with the RIM”) and Appendix II (“Derivation of component reliability targets from plant safety requirements”). Component Level Reliability Requirements will be derived from Plant Level Reliability Requirements through the Probabilistic Risk Assessment process. With Reliability Targets established, components will be assessed for mechanisms of environmental degradation and modes of failure as derived from the Phenomenon Identification and Ranking Table. Critical flaw size will be determined for the most likely modes of failure in each component. Monitoring and Non-Destructive Examination

technologies will be evaluated for the capability to detect sub-critical flaws and to endure the relevant inspection environments. Technologies and inspection schedules will then be selected for each area of interest to ensure that flaws can be detected before they grow to critical flaw size. Material performance will be monitored during operation, and data will be fed back to update the MANDE schedule throughout the life of the plant. The specific details of a RIM program for the KP-FHR will not be available in the near-term but will be provided with the Operating License application.

Surveillance Coupons

In-situ surveillance specimen programs have played an important role in materials degradation management in the Light Water Reactor industry since the 1970's and a similar program will be needed to validate our understanding of long-term material performance in the KP-FHR environment. In Light Water Reactors, one focus of the surveillance specimen program has been to monitor the degradation of fracture toughness of low-alloy steel reactor vessel materials with irradiation. Similarly, the surveillance specimen program for the KP-FHR will provide insight into the long-term combined effects of exposure to Flibe salt, irradiation, and high temperatures. A series of specimens will be strategically placed throughout the reactor vessel to provide coupons with a range of temperature and radiation exposure. These samples will be monitored throughout the life of the plant and assessed for changes in composition, phase stability, microstructure, and mechanical properties. These coupons will also be used to assess irradiation-affected corrosion, and irradiation-assisted stress corrosion cracking. The specific surveillance coupon program will be provided at the time of the Operating License application.

APPENDIX C. DATA ANALYSIS

Many testing programs that are expected to yield quantitative results and were developed with the intent of statistical analysis of the data. For example, the general corrosion testing of Alloy 316H and ER16-8-2 plans include three samples per condition, conducted over a wide range of times and temperatures. These data will be analyzed via electron microscopy of corrosion coupon cross sections which, we believe, is superior and more sensitive a measure than weight change.

With those corrosion data, Kairos Power will develop 'baseline' corrosion models for Alloy 316H and ER16-8-2 and conduct separate effects tests to assess key variables that include microstructure, contaminants, redox control, occluded geometry, and erosion-corrosion. Statistical analysis such as Analysis of Variance (ANOVA) will be used to establish the significance of these variables on the response model of corrosion rate compared to random error. Furthermore, the corrosion model will utilize appropriate prediction bands to ensure appropriate and conservative extrapolation from test conditions to KP-FHR operational times and temperatures.

Note that some testing may not be amenable to statistical analysis but is being performed to develop understanding and guidance. For example, the slow strain rate tests in Flibe are being performed primarily to assess regimes in which environmentally assisted cracking may occur. In these tests, a change in response (load vs. stroke) relative to air testing and post-test analysis of the fracture path will be used to develop understanding of the degree of concern for cracking. Similarly, stress corrosion cracking tests are being conducted to better understand if this phenomenon occurs in environments and mechanical conditions of relevance to the KP-FHR. Depending on the response of Alloy 316H and ER16-8-2 to these tests, a statistical analysis of the data may be used but also may employ fundamental materials science and engineering judgement to develop appropriate design factors or other practices (e.g. periodic inspection) that will appropriately address the concern of environmentally assisted cracking.

Note that corrosion rates can be confounded by complicating factors such as carbon pickup during testing as well as the difficulty in removing dried salt from test coupons. To mitigate these factors, Kairos Power will use electron microscopy of corrosion coupon cross sections as the primary method to assess corrosion (e.g. depth of chromium loss) as well as other compositional changes (e.g. the extent of Fe and Ni loss, the precipitation of Mo-rich Laves phase, and the precipitation of carbon rich phases). An example of this analysis is given below in Appendix C, Figure 1.

For information, an example of expected statistical analysis of corrosion data is presented below. In this example, the corrosion data of Zheng et al. (pink squares) are used to generate example corrosion data for three different temperatures and for times up to 10,000 hours (Reference 18). The example data are shown below in Appendix C, Figure 2.

An example of how these data may be fit is via Appendix C, Equation C-1. In Equation C-1, A is a fitting constant, t is the exposure time, n is a fitting constant (equal to 0.5 for mass diffusion control), Q is the apparent activation energy, R is the gas constant and T the temperature.

$$Cr\ loss\ depth = A * t^{n} * EXP(-Q/RT) \qquad \text{Eq. C-1}$$

The fit of the data to the combined model is shown by the blue surface in Appendix C, Figure 3. In this manner all the data (example date in gray circles, Zheng data in pink squares) can be used to increase the confidence in extrapolating to the conditions of the KP-FHR. For example, the reactor vessel will operate at approximately 550°C for [[ ]] which would exhibit <10 microns of corrosion (Cr loss) via the best estimate prediction of this model. The example baseline model is shown in two dimensions in Appendix C, Figure 4 (upper graph) with 95% prediction intervals. In Appendix C, Figure 4, an example of a separate effects corrosion test is shown (lower plot) along with how a factor of improvement may be defined. In this example, the factor of improvement is conservatively determined at an exposure time within the data and between the baseline model lower bound and the separate effects test upper bound.

Appendix C Figure 1. Example of How a Corrosion Coupon was Sectioned (left) and Corresponding Compositional Maps for Iron, Chromium, and Nickel

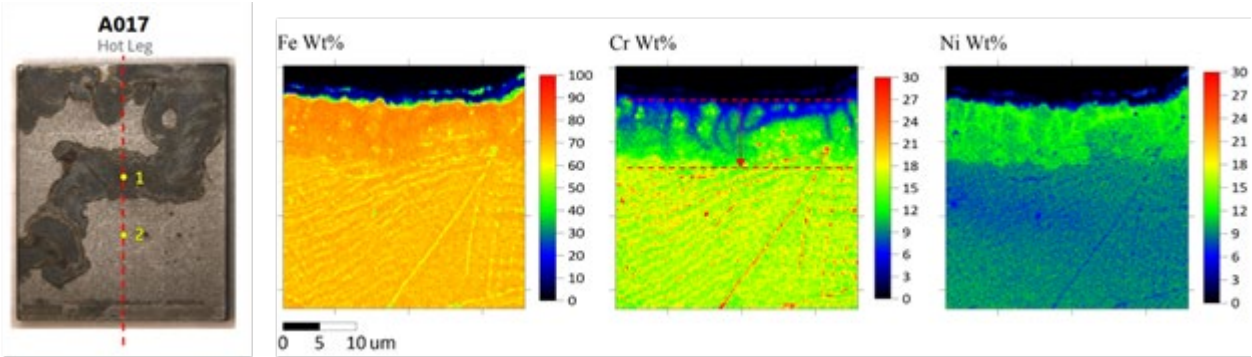

Appendix C Figure 2. The Corrosion Data of Alloy 316L in Flibe of Zheng (Pink Squares) Compared to Example Data at Three Different Temperatures

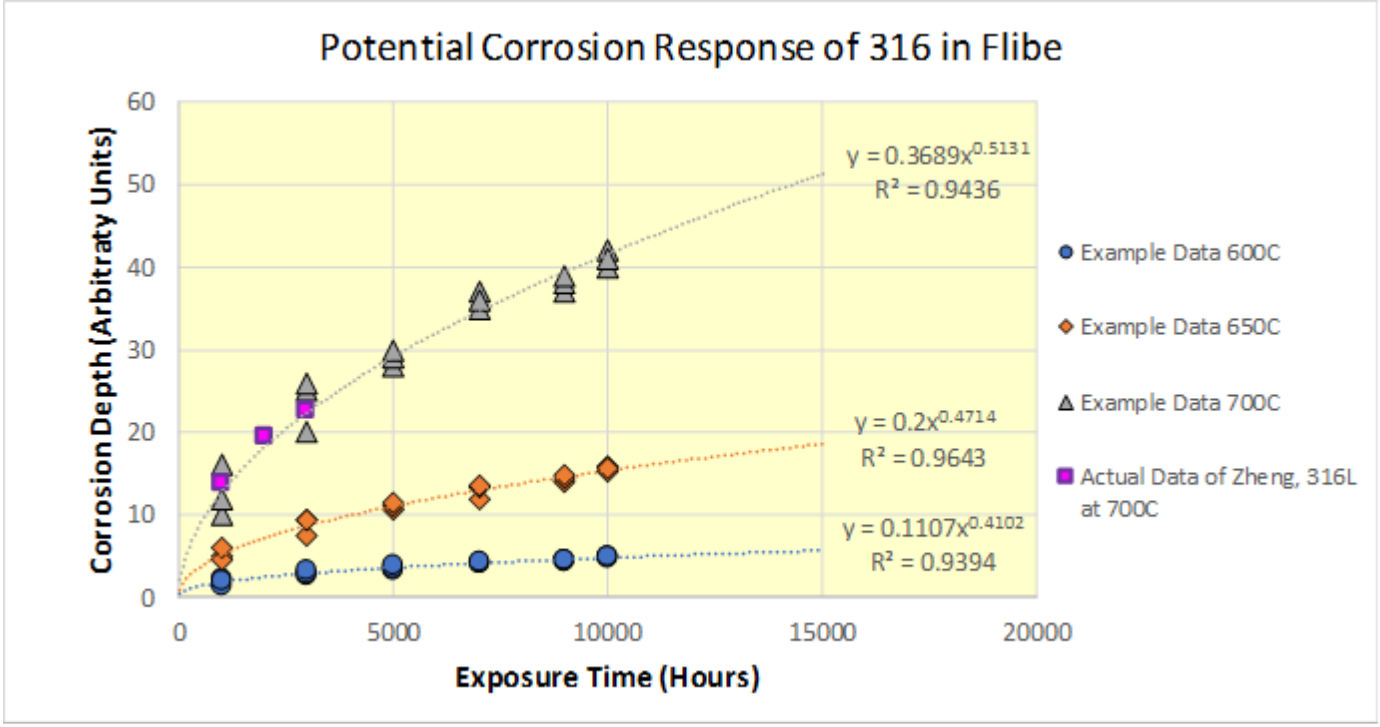

Appendix C Figure 3. Example of How Corrosion Data May be Fit and Extrapolated to Times Out to 20 years

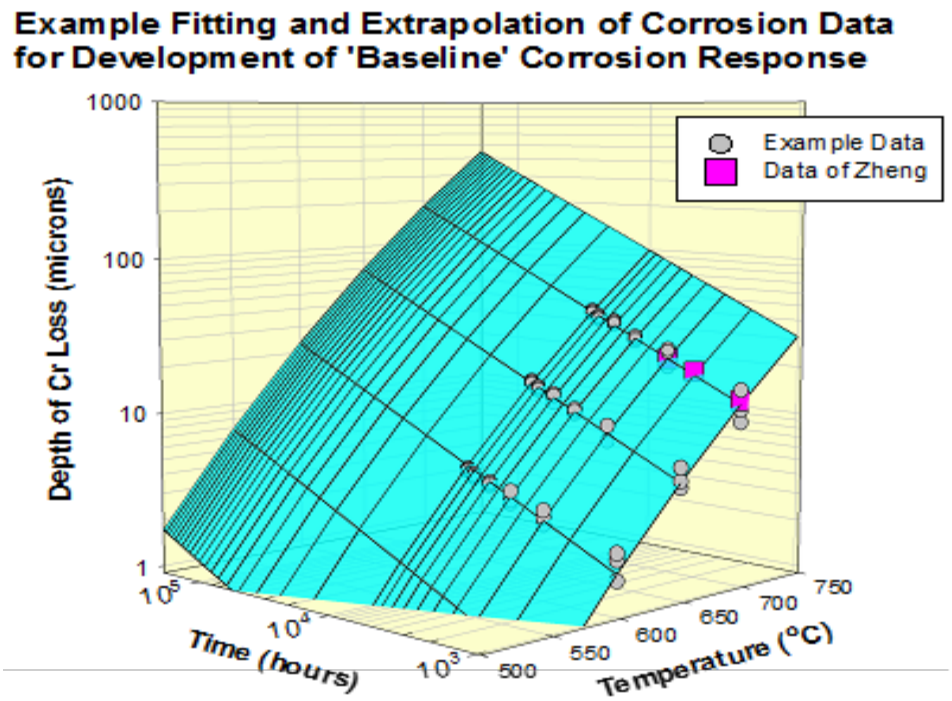

Appendix C Figure 4. Example of How the Baseline Corrosion Model May be Compared to a Separate Effects Test to Determine a Factor of Improvement

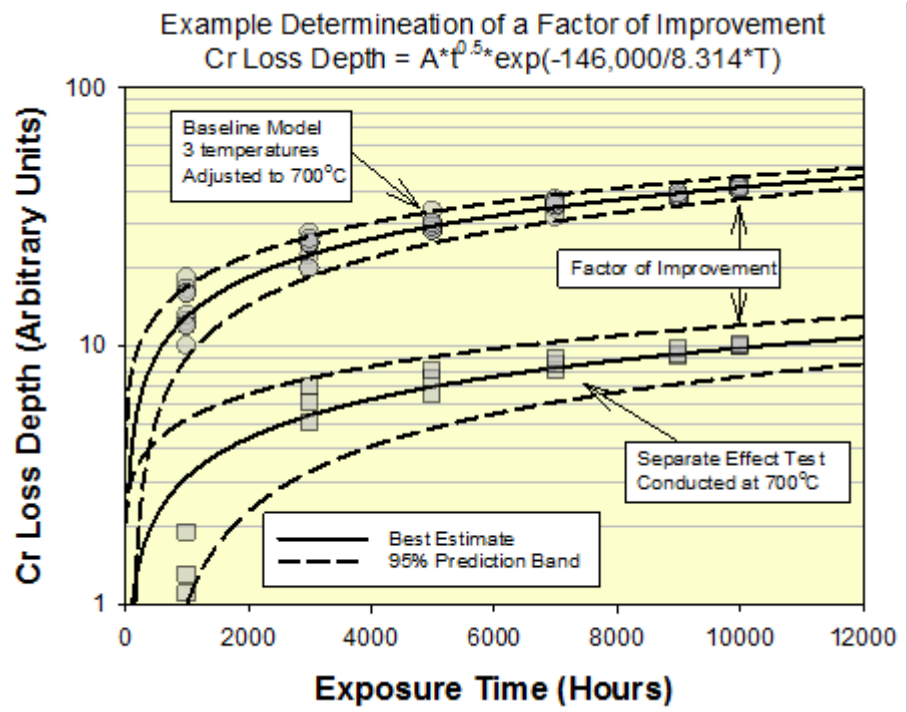

APPENDIX D. TEST SYSTEM DESIGNS FOR CORROSION AND ENVIRONMETALLY ASSISTED CRACKING

[[

Appendix D Table 1. Key Features of the Rotating Cage Loop Corrosion Test Systems

Appendix D Figure 1. Schematic Illustrations of the Rotating Cage Loop (upper) and In-Situ Mechanical Test Systems (lower)

]]

Enclosure 3

Affidavit Supporting Request for Withholding from Public Disclosure

(10 CFR 2.390)

Enclosure 3

Kairos Power LLC Affidavit and Request for Withholding from Public Disclosure (10 CFR 2.390)

I, Peter Hastings, hereby state:

1. I am Vice President, Regulatory Affairs and Quality at Kairos Power LLC ("Kairos"), and as such I have been authorized by Kairos to review information sought to be withheld from public disclosure in connection with the development, testing, licensing, and deployment of the Kairos reactor and its associated structures, systems, and components, and to apply for its withholding from public disclosure on behalf of Kairos.

2. The information sought to be withheld, in its entirety, is contained in Kairos' Enclosure 1 to this letter.

3. I am making this request for withholding, and executing this affidavit in support thereof, pursuant to the provisions of 10 CFR 2.390(b)(1).

4. I have personal knowledge of the criteria and procedures utilized by Kairos in designating information as a trade secret, privileged, or as confidential commercial or financial information. Some examples of information Kairos considers proprietary and eligible for withholding under §2.390(a)(4) include:

    a. Information which discloses process, method, or apparatus, including supporting data and analyses, where prevention of its use by Kairos competitors without license or contract from Kairos constitutes a competitive economic advantage over other companies in the industry;

    b. Information, which if used by a competitor, would reduce his expenditure of resources or improve his competitive position in design, manufacture, shipment, installation, assurance of quality;

    c. Information which reveals cost or price information, production capacities, budget levels, or commercial strategies of Kairos, its customers, its partners, or its suppliers;

    d. Information which reveals aspects of past, present, or future Kairos or customer funded development plans or programs, of potential commercial value to Kairos;

    e. Information which discloses patentable subject matter for which it may be desirable to obtain patent protection; and/or

    f. Information obtained through Kairos actions which could reveal additional insights into reactor system development, testing, qualification processes, and/or regulatory proceedings, and which are not otherwise readily obtainable by a competitor.

5. Information contained in Enclosure 1 to this letter contains details of Kairos Power's design and testing information intended to support NRC staff review. This information includes details of Kairos Power's design and testing plans that could provide a competitor with a commercial advantage if the information were to be revealed publicly.

6. Pursuant to the provisions of §2.390(b)(4), the following is furnished for consideration by the Commission in determining whether the information sought to be withheld from public disclosure should be withheld:

   a. The information sought to be withheld from public disclosure is owned and has been held in confidence by Kairos.

   b. The information is of a type customarily held in confidence by Kairos and not customarily disclosed to the public. Kairos has a rational basis for determining the types of information customarily held in confidence by it and, in that connection, utilizes a system to determine when and whether to hold certain types of information in confidence. The application of that system and the substance of that system constitute Kairos policy and provide the rational basis required.

   c. The information is being transmitted to the Commission in confidence and, under the provisions of 10 CFR 2.390, it is to be received in confidence by the Commission.

   d. This information is not readily available in public sources.

   e. Public disclosure of this proprietary information is likely to cause substantial harm to the competitive position of Kairos, because it would enhance the ability of competitors to provide similar products and services by reducing their expenditure of resources using similar project methods, equipment, testing approach, contractors, or licensing approaches. This information is the result of considerable expense to Kairos and has great value in that it will assist Kairos in providing products and services to new, expanding markets not currently served by the company.

   f. The information could reveal or could be used to infer price information, cost information, budget levels, or commercial strategies of Kairos.

   g. Each component of proprietary information pertinent to a particular competitive advantage is potentially as valuable as the total competitive advantage. If competitors acquire components of proprietary information, any one component may be the key to the entire puzzle, thereby depriving Kairos of a competitive advantage.

   h. Unrestricted disclosure would jeopardize the position of Kairos in the world market, and thereby give a market advantage to the competition in those countries.

I declare under penalty of perjury that the foregoing is true and correct.

Executed on: June 30, 2020

Peter Hastings

Vice President, Regulatory Affairs and Quality